



2014-11-01

Design Considerations in the Development and Actuation of Origami-Based Mechanisms

Eric W. Wilcox

Brigham Young University - Provo

Follow this and additional works at: <https://scholarsarchive.byu.edu/etd>



Part of the [Mechanical Engineering Commons](#)

BYU ScholarsArchive Citation

Wilcox, Eric W., "Design Considerations in the Development and Actuation of Origami-Based Mechanisms" (2014). *All Theses and Dissertations*. 5747.

<https://scholarsarchive.byu.edu/etd/5747>

This Thesis is brought to you for free and open access by BYU ScholarsArchive. It has been accepted for inclusion in All Theses and Dissertations by an authorized administrator of BYU ScholarsArchive. For more information, please contact scholarsarchive@byu.edu, ellen_amatangelo@byu.edu.

Design Considerations in the Development and Actuation of Origami-Based Mechanisms

Eric W. Wilcox

A thesis submitted to the faculty of
Brigham Young University
in partial fulfillment of the requirements for the degree of
Master of Science

Spencer P. Magleby, Chair
Larry L. Howell
Brian D. Jensen

Department of Mechanical Engineering
Brigham Young University
November 2014

Copyright © 2014 Eric W. Wilcox

All Rights Reserved

ABSTRACT

Design Considerations in the Development and Actuation of Origami-Based Mechanisms

Eric W. Wilcox
Department of Mechanical Engineering, BYU
Master of Science

Origami-based mechanisms have unique characteristics that make them attractive for engineering applications. However, origami-based design is still a developing area of design. Continued work to increase general understanding of key design parameters specific to origami-based mechanisms will increase the ability of designers to capture the potential benefits of origami-based mechanisms.

This thesis presents a fundamental study of origami to assist designers in gaining a stronger understanding of the key parameters and capabilities of origami-based mechanisms. As a starting point a study of fundamental motions in action origami models (those that exhibit motions in their folded state) is presented to explore fundamental motions and actuation in origami-based mechanisms. Eleven fundamental motions are outlined and defined with the associated actuation forces that drive them.

Additionally, considerations for ensuring necessary performance and force transfer characteristics in origami mechanisms are presented. This is done by exploring the effect of surrogate hinge selections, fold pattern modification, and actuation inputs on the final mechanism. A model of mechanical advantage in origami models consisting of N , degree-4, vertices (where $N = 1, 2, 3, \dots$) is developed and explored.

From the exploration of the parameters of the mechanical advantage model it is shown that hinge selection can greatly affect the performance of an origami mechanism by determining its range of motion, precision, and mechanical advantage. Therefore, in order to better understand this important design decision, specific considerations for surrogate hinge selection are presented. These considerations discuss methods to increase performance and reduce hinge imprint, as well as develop surrogate hinges in metals.

The key design parameters and considerations presented herein as well as study of origami motions serve to lay the groundwork toward the development of analysis tools and design guidelines specifically suited to origami based design.

Keywords: origami, fundamental motions, classification, mechanical advantage, practical design considerations, surrogate hinges

ACKNOWLEDGMENTS

As I consider the work and effort that has gone into this thesis, I am amazed at what I have been able to accomplish and recognize that it is only due to the support and help I had from those around me. This would not have been possible without them.

I would like to thank my committee, particularly Professor Magleby, for their support, direction, patience, and insights that have helped me come from initial concepts to this final product.

I would like to thank my fellow lab-mates Isaac Delimont, Jordan Tanner, Brandon Hanna, Ezekiel Merriam, and Thomas Evans. So much of this thesis has been shaped by the insights they have shared during the countless conversations we have had while working in the lab. I thank them for their willingness to brainstorm with me and serve as sounding boards as I tried to solidify theories or grasp new concepts.

I thank Brigham Young University for giving me the opportunity to be a part of their legacy of academic excellence. I thank them for their dedication to students that is demonstrated in their amazing facilities, incredible faculty, and wonderful learning environment.

Of course I must recognize the support I have had from my friends and family. I want to thank my best friend, Curtis Koelling, for the countless risk games that allowed me to relax from stressful weeks and long days as well as his contagious love for science which helped me maintain a healthy vision of what is possible when we put our minds to something.

I thank my parents, Darren and Tami, for the lessons of hard work and diligence they taught me - not only in word but in their daily example. I would not be who or where I am today without their guidance.

I thank my wife, BrookeLynne, for her love and support. Her faith in me, especially in those times where I felt stuck or inadequate, allowed me to rise above what I thought possible time and time again.

I thank my beautiful daughter, Avery, for the much needed study-breaks she gave me, as well as the lessons I have learned from her innocent, child-like, wonder at the world around her. She helps me to see the world for what it is: endless opportunities to learn and grow.

Finally, I am deeply grateful to my Heavenly Father. I have felt His influence as an illuminating light of knowledge and understanding. Some of the major developments in my research I attribute to His inspiration. For His help in this work, as well as His influence in all other areas of my life I am truly humbled and deeply grateful.

This thesis is based on work supported by the National Science Foundation and the Air Force Office of Scientific Research through NSF Grant No. EFRI-ODISSEI-1240417.

TABLE OF CONTENTS

LIST OF TABLES	vii
LIST OF FIGURES	viii
NOMENCLATURE	x
Chapter 1 Introduction	1
1.1 Motivation	1
1.2 Thesis Objective	2
1.3 Thesis Outline	2
Chapter 2 Exploring Movements and Potential Actuation in Action Origami	4
2.1 Introduction	4
2.2 Background	5
2.2.1 Important Terms	6
2.2.2 Classification of Models within Kinematic Origami	8
2.3 Approach	8
2.4 Discussion of Fundamental Origami Motions	9
2.4.1 Single	10
2.4.2 Coupled	13
2.4.3 N-long Linear Chain	17
2.4.4 Single Loop Network	20
2.5 Results	23
2.6 Conclusion	23
Chapter 3 Considering Mechanical Advantage in the Design of Origami-Based Mechanisms	25
3.1 Introduction	25
3.2 Background	26
3.3 Mechanical Advantage Model	27
3.3.1 Modelling a Single Origami Vertex	27
3.3.2 N Linearly-Linked Vertices	31
3.3.3 Key Parameters Affecting Mechanical Advantage	34
3.4 Key Parameters' Effect on Origami-based Design	38
3.4.1 Surrogate Hinges	38
3.4.2 Actuation Inputs	39
3.4.3 Fold Pattern Sector Angles	39
3.5 Conclusion	40
Chapter 4 Considerations for the Selection of Surrogate Hinges in Origami-Based Mechanisms	41
4.1 Introduction	41

4.2	Background	42
4.3	Practical Considerations Relating to Surrogate Hinge Selection	43
4.3.1	Surrogate Hinge Imprint	43
4.3.2	Required ROM of a Hinge	43
4.3.3	Increasing the Precision of a Hinge	44
4.3.4	Types of Loads on the Hinges	44
4.4	Selection of Surrogate Hinges in Metals	45
4.4.1	Network Hinges	45
4.4.2	Systems of Network Hinges	46
4.5	Conclusions	47
Chapter 5	Conclusion	49
5.1	Conclusions	49
5.2	Future Work	50
	REFERENCES	51

LIST OF TABLES

2.1	Summary of characteristic motions and actuation inputs for each subset.	24
-----	---	----

LIST OF FIGURES

2.1	The backbone (dashed line) of Single, Coupled, and N-Long Linear Chain type mechanisms.	6
2.2	A partially folded single vertex with the ground plane indicated in grey.	7
2.3	Crease patterns for Subsets S1 (a) & S2 (b) of the Single class.	9
2.4	Applied forces (blue arrows) that create the output (red arrow) of Subset S1a - a moment about the backbone (dashed line) or forces applied orthogonally to the backbone plane.	10
2.5	Traditional Flapping Crane showing buckled panels.	11
2.6	Input force requirements (blue arrows) to create output (red arrows) of Subset S2.	12
2.7	A waterbomb base belonging to Subset S3 shown moving between its two stable positions by inverting the fold vertex.	13
2.8	Typical crease patterns from each of the three subsets of the Coupled class: Subset C1 (a), Subset C2 (b) & Subset C3 (c).	14
2.9	Actuation of a fold pattern belonging to Subset C1, showing input forces (blue arrows) and the resulting output motion (red arrows).	14
2.10	Actuation of a fold pattern belonging to Subset C2 with input forces (blue arrows) and output motions shown (red arrows).	15
2.11	Extension motion created in a C2 type fold by actuating the panels at the extreme end of the backbone.	15
2.12	Actuation of a fold pattern belonging to Subset C3 showing output motion (red arrows) and the input forces that create it (blue arrows).	16
2.13	Linear extension created in a C3 type fold with parallel guiding action of the extreme ends of the backbone.	16
2.14	Crease patterns for LC1 (a) and LC2 (b) subsets of the N-Long Linear Chain class with fold pattern backbones indicated (dashed lines) and input forces shown (blue arrows).	17
2.15	Extension/contraction motion of Subset LC1 (red arrows) created by applying a moment about the backbone.	18
2.16	A fold pattern belonging to Subset LC2 showing the kinked backbone (solid red), linear pseudo-backbone (dashed-red), and extension/contraction output motion (red arrows).	19
2.17	Crease patterns belonging to Subsets SL1 (a) and SL2 (b) showing the direction of the center loop's rotation.	20
2.18	A hexagonal flasher belonging to Subset SL1 showing in-plane rotation of the central loop and radial expansion motions of the flasher as well as the direction and location of the forces that create them (blue arrows).	21
2.19	Output motion (red arrow) of Subset SL2 showing the out-of-plane rotation of the center loop (outlined in red).	22
3.1	Origami vertex (shown in grey) with an equivalent rigid-body spherical mechanism and the axes of its revolute joints (shown in blue).	26

3.2	General degree-4 vertex in flat (a) and folded (b) states with sector and dihedral angles labeled with α and θ respectively. Fold assignments are indicated in (a) with dashed red (valley) and solid black (mountain).	28
3.3	MA_r vs. MA_c for a degree-4 vertex with sector angles $\alpha_1 = \frac{2\pi}{3}$, $\alpha_2 = \frac{2\pi}{3}$, $\alpha_3 = \frac{\pi}{3}$, and $\alpha_4 = \frac{\pi}{3}$. The MA_c curve is calculated with $M_{in} = 0.113$ Nm and $k = 0.178$ Nm/radian.	30
3.4	Example of a linear-linked origami fold pattern shown both flat (a) and partially folded (b). Fold assignments are indicated in (a) with dashed red (valley) and solid black (mountain).	31
3.5	MA_r vs. MA_c for a mechanism consisting of two, linearly-linked, degree-4 vertices with sector angles $\alpha_1 = \frac{2\pi}{3}$, $\alpha_2 = \frac{2\pi}{3}$, $\alpha_3 = \frac{\pi}{3}$, and $\alpha_4 = \frac{\pi}{3}$. The MA_c curve is calculated with $M_{in} = 0.113$ Nm and $k = 0.178$ Nm/radian.	33
3.6	Effect of compliant hinge stiffness (k) on mechanical advantage of a degree-4 vertex with $M_{in} = 0.113$ Nm.	35
3.7	Effect of input force (M_{in}) on mechanical advantage of a degree-4 vertex where $k = 0.890$ Nm/radian.	36
3.8	Effect of the sector angles (α) in a degree-4 origami vertex on mechanical advantage. Here α_2 is modified from its nominal value of $\frac{2\pi}{3}$ (red). Hinge stiffness and actuation input are: 0.222 Nm/radian and 0.113 Nm respectively.	38
4.1	Example orientations of network hinges connected in parallel and series. Rigid panels are shown with hash marks and network hinges with solid fill.	46
4.2	Stacked orientation of serially connected network hinges with overall hinge deflection and individual network hinge deflection angles shown.	47

NOMENCLATURE

α_i	Origami vertex sector angle of panel i
γ_i	Exterior dihedral angle between panels i and $i+1$
k	Equivalent torsional stiffness of a compliant joint
MA_c	Mechanical advantage of a mechanism with compliant segments
MA_r	Kinematically predicted mechanical advantage of a rigid-body mechanism
θ_i	Interior dihedral angle between panels i and $i+1$
θ_{i_0}	Undeformed angle for compliant hinge, i , between panels i and $i+1$

CHAPTER 1. INTRODUCTION

1.1 Motivation

Origami models exhibit many behaviors that are desirable for use in engineering applications such as reconfigurability, high compactibility, and the ability to be manufactured from a single sheet. Their unique set of characteristics make them a useful source of inspiration for designers and are being used to create unique solutions to engineering problems. The widespread use of origami-based mechanisms is still limited, however, by the difficult nature of moving from seed origami model to final, actuated, mechanism.

The first difficulty in this process is selecting the appropriate origami fold pattern to begin the design. A better understanding of fundamental origami motions and how to actuate them can assist in the effective selection of origami models from which to develop the origami-based mechanism.

Once a starting point has been selected for a mechanism, there are additional design decisions to be made that will greatly affect the final performance and behavior. Increased understanding of some of these critical design decisions and how they determine the behavior of the mechanism will allow designers to troubleshoot difficult aspects of the origami-based design process.

Some potential applications for origami-based mechanisms are beyond current capabilities due to the limitations inherent in the materials from which they are constructed as well as those imposed by the hinges being used. The ability to produce fully compliant, origami-based mechanisms in materials with greater strength, corrosion resistance, etc. and with greater hinge performance will further increase the possible applications of these mechanisms.

Origami-based mechanisms have unique and desirable characteristics and offer novel solutions to engineering problems. By establishing a fundamental understanding of achievable motions, understanding critical design parameters, and exploring the use of materials such as metals in

the design of origami-based mechanisms; the development of mechanisms with greater complexity and possible application will be facilitated. This in turn will broaden the use of origami-based mechanisms and allow more designers to take advantage of their benefits.

1.2 Thesis Objective

The purpose of this thesis is to assist in the effective synthesis of compact, deployable, and highly compactable origami-based mechanisms. This is performed by first investigating and classifying action origami models by their fundamental motions and required actuation inputs, then exploring key parameters controlling the force-deflection behavior of origami-based mechanisms and finally discussing practical considerations affecting the performance of the compliant hinges used in origami-based mechanisms. Included is a discussion of specific considerations when developing such hinges in metals.

1.3 Thesis Outline

In Chapter 2, the fundamental motions exhibited by action origami models are outlined and required actuation inputs discussed. Over 300 action origami models are classified based on their spherical mechanism structure and motions, resulting in 11 different categories. This chapter has been published in the proceedings of the 2014 Design and Engineering Technical Conferences (DETC) [1].

Chapter 3 presents a mechanical advantage model for flat folding, rigidly foldable, linearly-linked origami fold patterns consisting of N degree-4 vertices (where $N=1,2,3\dots$). This mechanical advantage model is used to explore and identify critical design parameters affecting the performance of origami-based mechanisms. Discussion of these key parameters allows designers of origami-based mechanisms to gain a better understanding of their effect on the performance of origami-based mechanisms. This chapter has been submitted for publication in the Journal of Mechanical Design.

Chapter 4 discusses practical considerations concerning the selection of surrogate hinges for origami-based mechanisms, as this was shown in Chapter 3 to be one of the more critical pa-

rameters affecting their performance. Considerations to be made in order to increase performance, reduce hinge imprint, and create hinges in low compliance materials (metals) are discussed.

Lastly, Chapter 5 includes conclusions drawn from the research as well as areas of future work.

CHAPTER 2. EXPLORING MOVEMENTS AND POTENTIAL ACTUATION IN ACTION ORIGAMI

2.1 Introduction

There has been a growing interest in origami-inspired mechanisms. The design of these mechanisms draws from the vast repertoire of origami models to create innovative solutions to unique and challenging problems in applications as diverse as medical equipment [2], aircraft construction [3], and space applications [4]. With the application of mathematical modeling and analysis, origami designs have grown in complexity. These increasingly advanced origami models promise to serve as useful tools in the creation of engineering solutions to equally specialized and unique design problems. However, as origami models grow in complexity there is a greater need for actuators that will meet the specific requirements of the resulting mechanisms. This presents an opportunity for the development of origami-compatible actuators catering to the design space of origami-inspired mechanisms. For instance, in designs where volume must be minimized, conventional actuators may not be appropriate as they add unwanted bulk. In such circumstances origami-compatible actuation systems designed to address this need could be selected to create the needed movements without compromising performance. In this way the fields of actuation and origami-inspired mechanisms are connected. Actuation technology is already being developed to create actuation systems with less bulk, more autonomy, and greater control [5–7].

To efficiently advance the development of origami-compatible actuator systems, it is important to first understand the types of motion exhibited by origami models. In conventional engineering designs, the motion of a given mechanism is a combination of the simple movements of its components. These movements and how they couple together to form more complex motions are well-documented and understood, allowing engineers to create sophisticated motion. Gaining a similar understanding of the fundamental movements in origami models is an important step in creating fully actuated origami-inspired mechanisms. The objective of this chapter is therefore to

define the fundamental motions in origami and identify the actuation inputs required to achieve these motions in origami-inspired mechanisms.

2.2 Background

Origami can be split into static and action origami models. Static origami consists of models that exhibit no motion once folded. While such models can be complex and visually stunning, it is difficult to translate their design into use in mechanisms. In contrast, action origami models can be more directly translated into use in creating mechanisms due to their ability to create motion in their folded state.

Some action origami models exhibit motions that cannot be predicted or replicated using traditional kinematics, making them difficult to recreate in mechanisms. Thus designers may find it useful to focus on models whose motions can be defined by rigid-body kinematics. Such models have been defined as “kinematic action origami” [8]. Kinematic action origami models are designs that can be modeled as mechanisms with relative motion between components and a distinct output motion from a given input.

Modeling origami fold patterns as kinematic mechanisms is well established in papers considering the behavior of origami folds [9–12]. Each vertex is modeled as a spherical center to an equivalent spherical mechanism with the surrounding panels acting as rigid links and fold lines acting as revolute joints. Bowen et al. [8] proposed classes into which the kinematic origami models could be further divided by considering the driving fold pattern of the model. The driving fold pattern of a model is the network of fold lines and vertices *directly* involved in creating the motion of the model. The proposed classification scheme analyzed how each vertex in the driving fold pattern interacted spatially with the vertices around it. This chapter’s study of the motions exhibited in several of these classes will serve to define fundamental types of motions observed in kinematic origami models. Once an understanding of such motions and their actuation has been established, further study could show how these basic building blocks can be combined to create the more complicated motions exhibited in the other classes not addressed here.

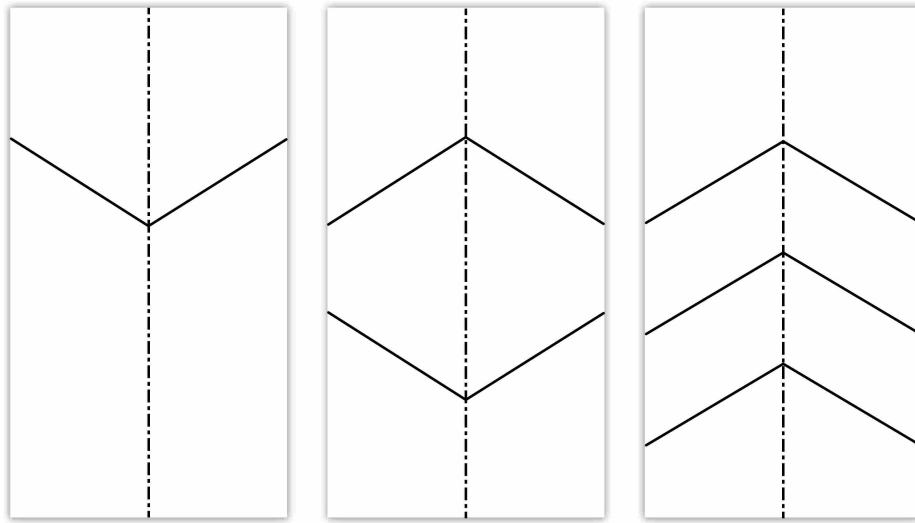


Figure 2.1: The backbone (dashed line) of Single, Coupled, and N-Long Linear Chain type mechanisms.

2.2.1 Important Terms

A brief explanation of important terms used in the following discussion is provided below.

Rigid Foldability: An origami model is rigidly foldable if the panels between folds remain rigid and planar throughout the entire motion of the model (i.e. there is no flex in the panels).

Spherical Center: The spherical center is the point in space where the rotational axes of each of the revolute joints of a spherical mechanism intersect. By considering origami fold lines to be the axis of a revolute joint their point of intersection at the vertex can be modeled as the spherical center of an equivalent spherical mechanism.

Sector Angle: The sector angle of a given panel in an origami vertex is the enclosed angle of that panel measured between the creases that intersect with the origami vertex. In the context of spherical mechanisms the sector angle is equivalent to the spherical link length for that panel.

Backbone: The backbone is a fold line that connects all spherical centers in the fold pattern being considered. Figure 2.1 shows crease patterns for Single, Coupled, and N-Long Linear Chain

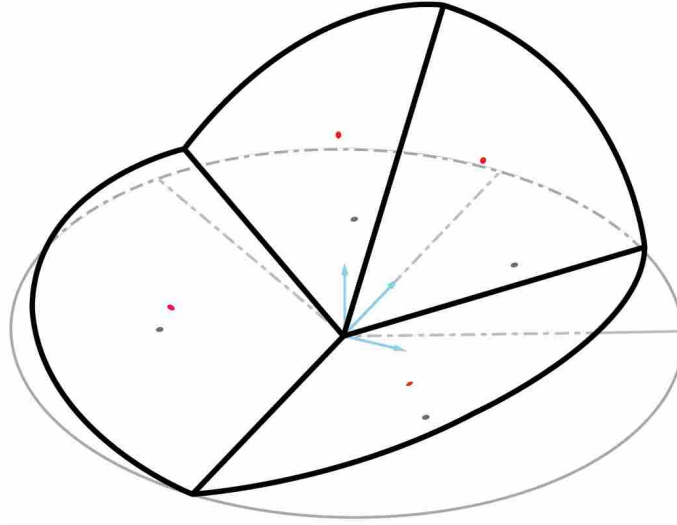


Figure 2.2: A partially folded single vertex with the ground plane indicated in grey.

type fold patterns with their respective backbones indicated. The concept of a backbone is only applicable to open-chain type fold patterns.

Ground Plane: Here the ground plane is defined as the plane the origami fold pattern lies in when completely unfolded. As an origami folding pattern is actuated, the segment of the backbone lying between the driving panels (where the actuation forces are being applied) remains in the ground plane while the rest emerges out of the ground plane. A partially folded single vertex is shown in Figure 2.2 with the ground plane indicated. Notice also the segment of the backbone that remains in the ground plane throughout the entire motion.

Backbone Plane: The backbone plane for a given origami folding pattern is the plane which contains the backbone of the folding pattern and remains perpendicular to the ground plane.

Back-Drivability: In this study the term “back-drivable” describes origami fold patterns whose output motion can be actuated to recreate the input motion required to create it. For example, a model requiring a linear translation of panels to create a rotational output is back-drivable if and only if applying actuation forces to the panels involved in the output motion recreates the translation motion of the panels involved in the input motion.

An origami fold pattern is considered to be back-drivable if it is rigidly foldable and can be modeled as a 1 DOF kinematic system. However, while a system may be back-drivable in theory it may prove difficult to realize in practice. For this reason, the practicality of back-driving some of the fold patterns is also considered.

2.2.2 Classification of Models within Kinematic Origami

In this chapter we have chosen to focus on four of the classes proposed for action origami by Bowen et al. [8]. Each is defined briefly below.

Open Chains

Single. A model whose driving fold pattern creates only one spherical mechanism.

Coupled. A model with a driving fold pattern containing two spherical mechanisms that are coupled such that they share one joint.

N-Long Linear Chain. A model with three or more spherical mechanisms linked linearly such that each spherical mechanism will share two joints, one with each of the neighboring spherical mechanisms in the chain. The spherical mechanisms located at the extreme positions of the chain will only share one joint with the adjacent spherical mechanism in the chain.

Networks

Single Loop. A model with a fold pattern that has only one loop (closed chain of at least 3 spherical centers) and where all spherical mechanisms in the loop share two joints.

2.3 Approach

The classes of origami models being considered here will be analyzed in order to characterize the motions created by each type of driving fold pattern discussed. Subsets representing fundamental types of motions in kinematic origami models will be outlined and placed inside the framework of the existing classification scheme [8]. These subsets will be defined by:

- 1) Motions exhibited
- 2) Types of actuation forces required
- 3) Back-Drivability

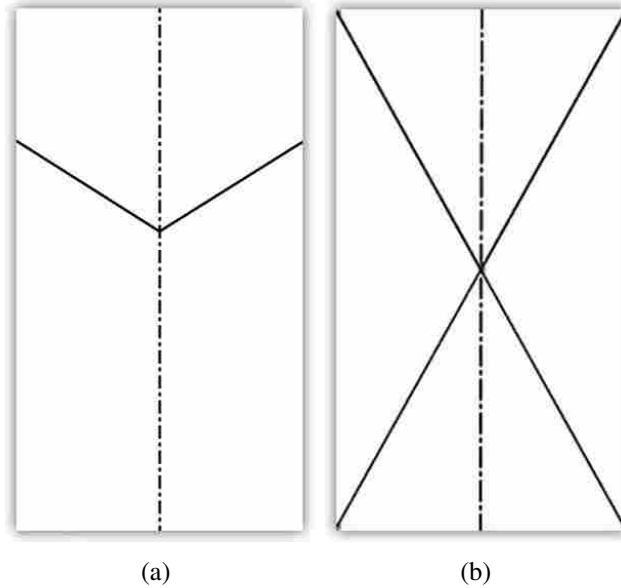


Figure 2.3: Crease patterns for Subsets S1 (a) & S2 (b) of the Single class.

Results of the study are summarized for each subset in Table 2.1 at the conclusion of this chapter. The table is intended as a quick-reference tool for designers of origami-inspired mechanisms or others seeking to better understand the movements and actuation of kinematic origami models.

Robert Lang and Jeremy Shafer, well known origami artists, have created many action origami models and their books were the sources of the origami models discussed in this chapter [13–16]. Approximately 140 kinematic origami models were analyzed. In studying these models only the fold patterns from each design that were directly involved in driving the motion of the model were considered.

This chapter is intended as an introduction to the basic types of motions in kinematic action origami. The statements made concerning each subset are intended to be generic to apply to all models in each group.

2.4 Discussion of Fundamental Origami Motions

This discussion starts with models in the Single class [8] by outlining subsets in this class and then outlining subsets in the Coupled, N-Long Linear Chain, and Single Loop classes.

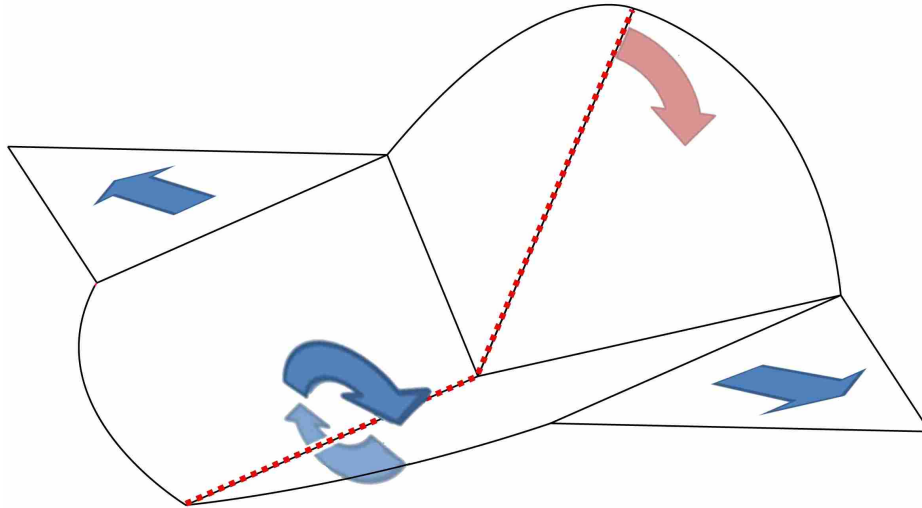


Figure 2.4: Applied forces (blue arrows) that create the output (red arrow) of Subset S1a - a moment about the backbone (dashed line) or forces applied orthogonally to the backbone plane.

2.4.1 Single

The Single spherical mechanism class can be divided into four distinct subsets: Subset S1a, Subset S1b, Subset S2, and Subset S3. Subsets S1a and S1b consist of degree 4 vertex folds while Subsets S2 and S3 consist of folds with degree 6 (or greater) vertices. Further description of each subset is given below.

Subset S1a

This subset is the most basic of the Single class. Crease patterns associated with this subset, as shown in Figure 2.3(a), create degree 4 vertices – meaning the fold pattern can be represented by a 4R 1 DOF spherical mechanism. From the crease pattern one sees two sets of panels: one whose sector angles are less than 90° and another whose sector angles are greater than 90° . While either set of panels could be used to drive the motion of the model (as it is a 1 DOF system), here the panels whose sector angles are greater than 90° are referred to as “driving panels”. Actuation of these driving panels causes the other panels to rotate out of the ground plane.

Figure 2.4 shows the type of forces that can be applied to create the motion of Subset S1a: either a moment about the backbone or forces oriented perpendicular to the backbone plane and acting in a plane that remains parallel to the ground plane of the fold vertex (as defined earlier)

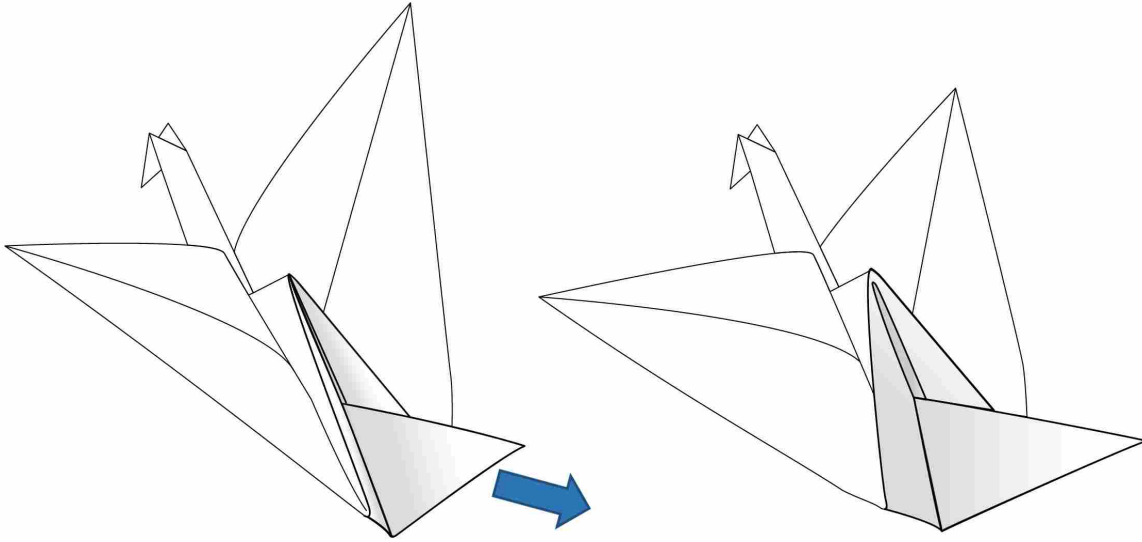


Figure 2.5: Traditional Flapping Crane showing buckled panels.

throughout the entire motion of the panels. This constraint is often realized in origami designs by attaching flaps to the panels being actuated and pulling on these flaps.

When using external flaps to actuate the fold pattern, the stroke length is determined by the vertical distance of the plane containing the flaps from the ground plane; as the distance decreases so will the stroke length. This statement applies to any fold pattern being actuated in this way. The output displacement of the fold pattern can also be changed by modifying the sector angle of the driving panels. As the angle of these panels approaches (but is still greater than) 90° the displacement is increased. The motion of this subset is back-driven by applying a moment about the backbone between the panels whose sector angles are less than 90° .

Subset S1b

The crease patterns associated with this subset are no different from that for Subset S1a given in Figure 2.3(a). The different motion behavior of the two subsets arises from the difference in actuation inputs applied to the fold pattern. This can be seen by considering the “Flapping Crane” [13, 15] shown in Figure 2.5. Models belonging to this subset gain their motion from pulling on two of the panels of the vertex such that the other panels buckle or flex as shown in Figure 2.5.

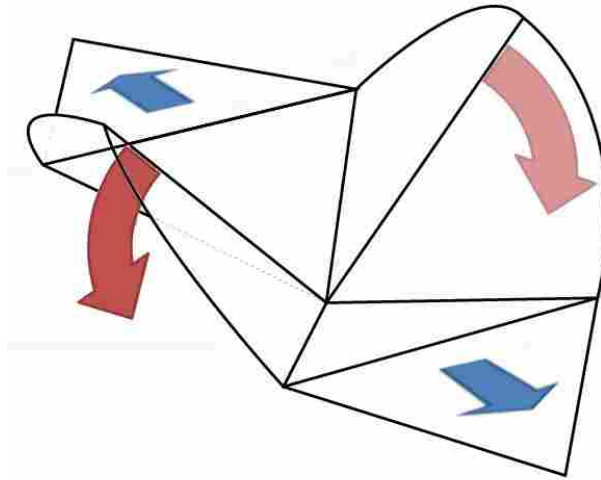


Figure 2.6: Input force requirements (blue arrows) to create output (red arrows) of Subset S2.

In this figure the single vertex is located in the tail section of the crane and actuation forces are applied to the panels with sector angles less than 90° , causing the others to buckle and create the flapping motion of the crane. While the tail section could be actuated as discussed with Subset S1a the characteristic flapping of the “Flapping Crane” would not be achieved; this motion is only created by the buckling and flexing of the panels in the tail section. Origami designs belonging to this subset are not rigidly foldable. A mechanism using a non-rigidly foldable design would require compliant links to function. Resulting actuation challenges arising from the use of compliant links could include the actuator being required to output a greater force as well as being required to resist a static load from the panels attempting to return to an un-flexed state. Also, due to the fold pattern being non-rigidly foldable, this motion is not back-drivable.

Subset S2

Subset S2, while similar to Subset S1a, has some important differences which can be seen in the crease pattern given in Figure 2.3(b). The most notable difference is that this crease pattern creates a degree 6 vertex which will have more than one degree of freedom. The output motion of the subset is similar to that of Subset S1a but differs in that the out-of-plane rotations occur on both sides of the panels driving the motion. Actuation forces are applied to the two center panels in the fold pattern (through the use of external flaps). The motion is created by forces applied

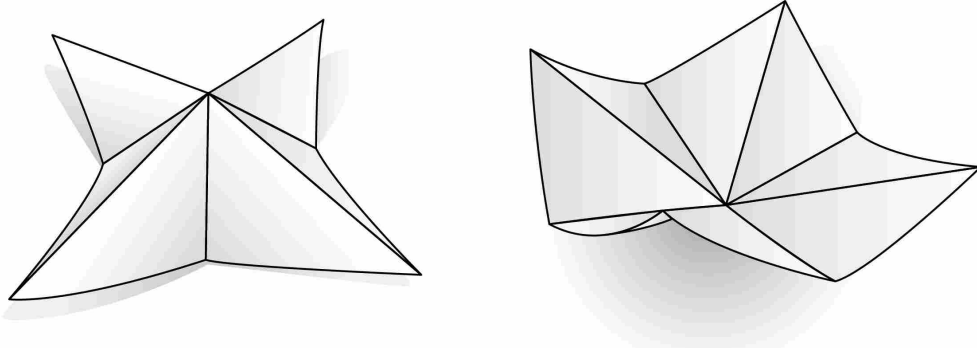


Figure 2.7: A waterbomb base belonging to Subset S3 shown moving between its two stable positions by inverting the fold vertex.

perpendicular to the backbone plane of the mechanism as demonstrated in Figure 2.6. As fold patterns belonging to this subset are not 1 DOF systems this subset is not back-drivable.

Subset S3

Subset S3 may be of particular interest to designers of origami inspired mechanisms as its motion demonstrates bistability which offers the potential benefit of lowering actuation energy requirements. The motion associated with this subset is an inverting of the vertex with the model moving between two stable positions as demonstrated in Figure 2.7. Any crease pattern with a single vertex containing at least four fold lines can exhibit this bistable behavior (although to be rigidly foldable at least six are required). Actuation of origami fold patterns in this subset can be difficult if attempting to invert the vertex by applying a force directly to it. An alternate actuation approach involves translational sliding contact on the mountain folds until the vertex pops through to its second stable position. This motion is not back-drivable.

2.4.2 Coupled

The Coupled mechanism class is the next evolution in mechanism complexity and is comprised of fold patterns in which two spherical mechanisms are coupled together. There are three possible orientations for the coupling of these spherical mechanisms which constitute the three subsets of this class. Crease patterns showing these three orientations are given in Figure 2.8. In the first subset (Subset C1) of coupled mechanisms the individual spherical mechanisms are

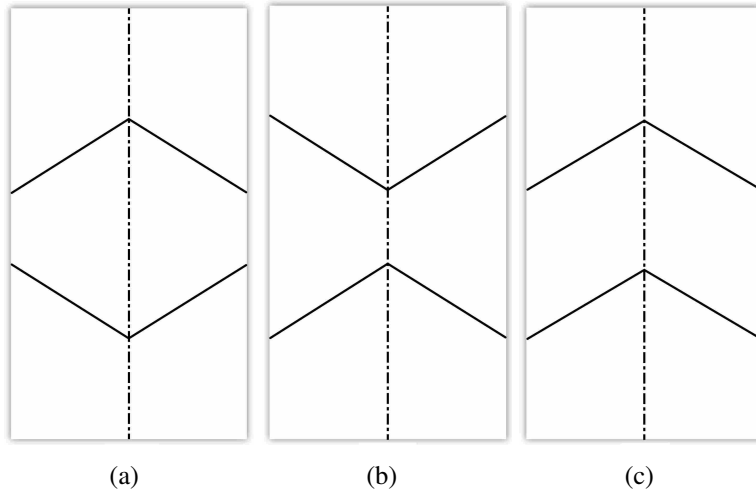


Figure 2.8: Typical crease patterns from each of the three subsets of the Coupled class: Subset C1 (a), Subset C2 (b) & Subset C3 (c).

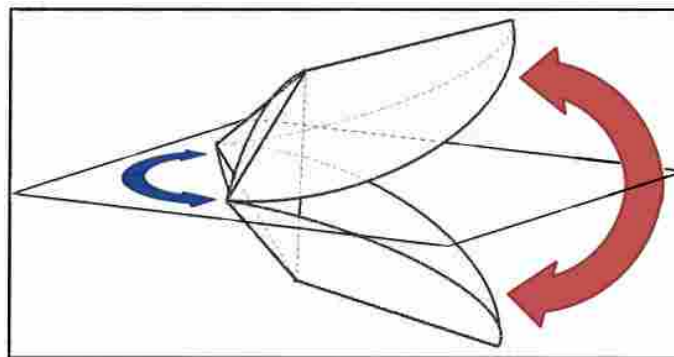


Figure 2.9: Actuation of a fold pattern belonging to Subset C1, showing input forces (blue arrows) and the resulting output motion (red arrows).

oriented towards each other (forming a diamond), in the second subset (Subset C2) the two spherical mechanisms are oriented away from each other, while in the third (Subset C3) the spherical mechanisms are oriented in the same direction. These subsets are described below.

Subset C1

This subset is the most populated of any of the Coupled subsets and is seen in many action origami models – particularly in those exhibiting chomping motions. The crease pattern associated with this subset is shown in Figure 2.8(a). As described earlier the two spherical mechanisms are

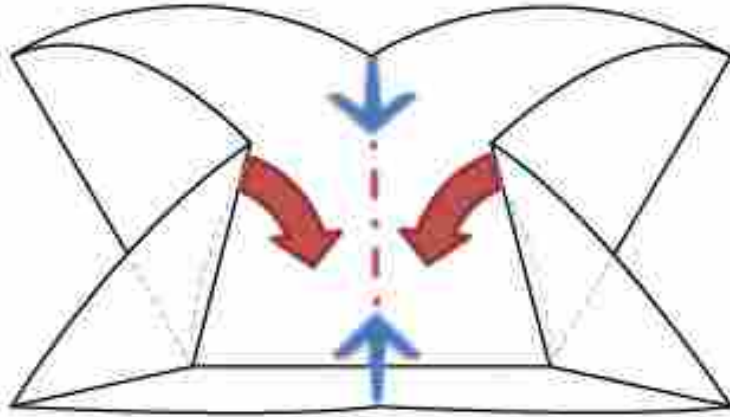


Figure 2.10: Actuation of a fold pattern belonging to Subset C2 with input forces (blue arrows) and output motions shown (red arrows).

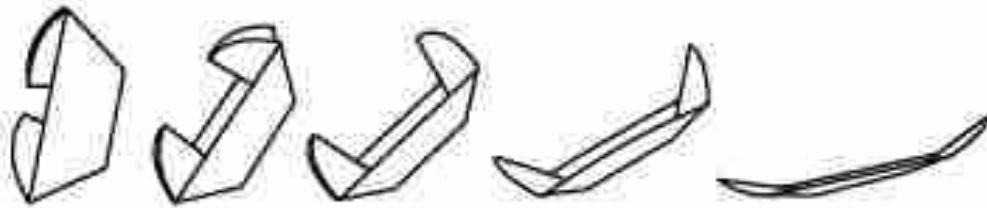


Figure 2.11: Extension motion created in a C2 type fold by actuating the panels at the extreme end of the backbone.

oriented towards each other such that a diamond shape is created in the middle of the fold pattern. The chomping motion of this subset, as shown in Figure 2.9, is actuated by bringing the points of the “diamond” together in one plane causing the extreme endpoints of the backbone to be brought together in an orthogonal plane. This motion can be initiated by applying a moment to the panels of the diamond about the backbone (possibly with the use of forces on flaps as discussed earlier) or by applying a moment about the fold line in the middle of the diamond. This motion is back-driven by bringing the extreme points of the backbone together in one plane causing the points of the diamond to come together in an orthogonal plane.

Subset C2

Subset C2 of the Coupled class is characterized by coupled spherical centers which are oriented away from each other as shown in the crease pattern in Figure 2.8(b). This subset is

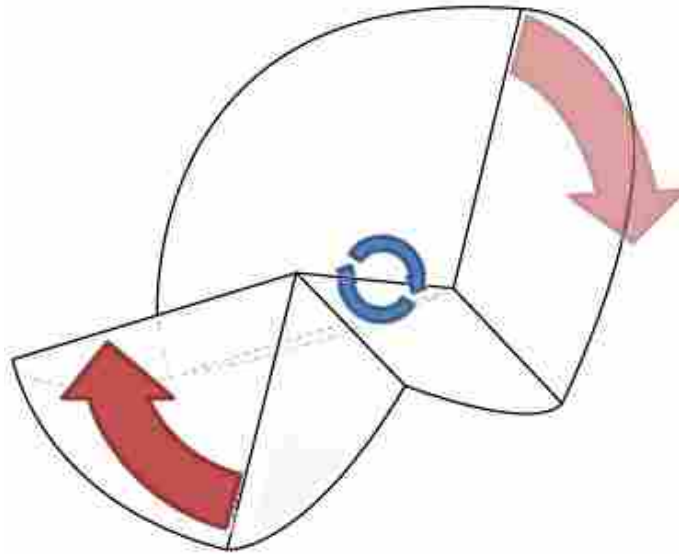


Figure 2.12: Actuation of a fold pattern belonging to Subset C3 showing output motion (red arrows) and the input forces that create it (blue arrows).

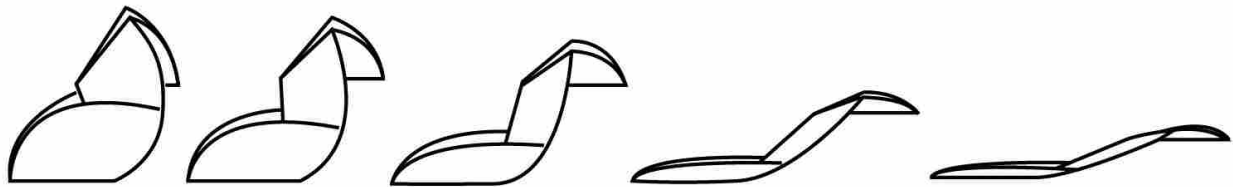


Figure 2.13: Linear extension created in a C3 type fold with parallel guiding action of the extreme ends of the backbone.

actuated as the center panels move together causing the two extreme points of the backbone to move together as shown in Figure 2.10. Like Subset C1, this motion is actuated by a moment about the backbone applied to the input panels. Depending on the panels selected as input the fold pattern will generate motion as shown in Figure 2.10 or, by actuating a set of panels at one of the extreme ends of the backbone, an extension type motion as shown in Figure 2.11. These motions are back-drivable.

Subset C3

This subset is not commonly represented in origami designs but consists of crease patterns where the the two coupled spherical centers are oriented in the same direction (see Figure 2.8(c)).

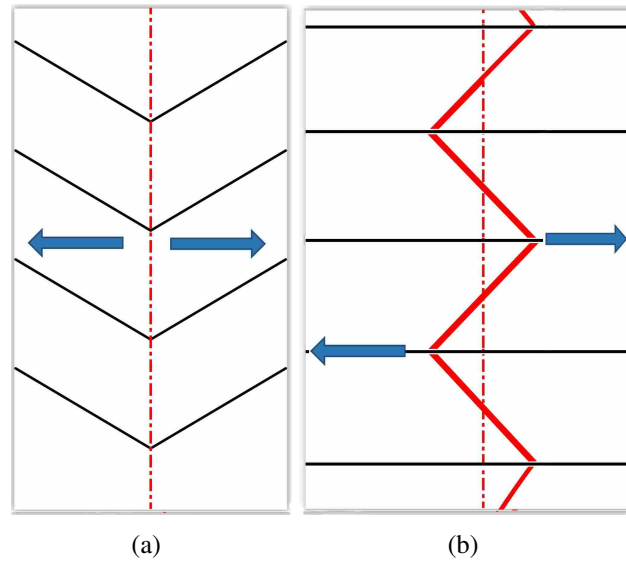


Figure 2.14: Crease patterns for LC1 (a) and LC2 (b) subsets of the N-Long Linear Chain class with fold pattern backbones indicated (dashed lines) and input forces shown (blue arrows).

Actuation of the fold pattern is accomplished by applying a moment about the center segment of the backbone, creating a rotation of the end segments of the backbone as shown in Figure 2.12. This fold pattern is back-driven by actuating a set of panels at one of the end segments of the backbone. An interesting feature of this subset is that by actuating the extreme panels in the mechanism a simple parallel guiding mechanism is created as the extreme ends of the backbone remain parallel throughout the entire motion (see Figure 2.13).

2.4.3 N-long Linear Chain

The next level in mechanism complexity is the N-Long Linear Chain class. For this class there are two subsets: Linear (LC1) or Kinked (LC2). Crease patterns from each subset are given in Figure 2.14. The first subset consists of fold patterns that have a linear backbone while the other has a kinked backbone that zig-zags across a linear “pseudo-backbone”. The specific movement characteristics can vary depending on the types of folds branching from the backbone and their orientations relative to each other, however a few general statements can be made about the movements of this class as discussed below.

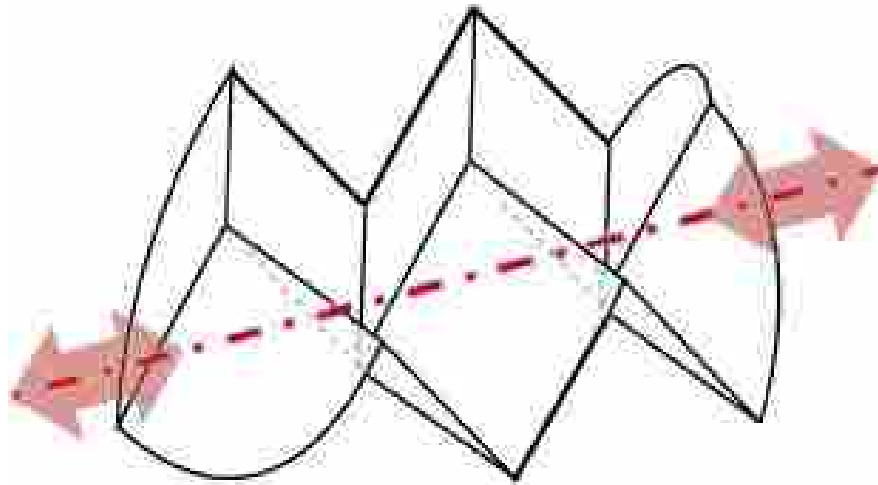


Figure 2.15: Extension/contraction motion of Subset LC1 (red arrows) created by applying a moment about the backbone.

Subset LC1 - Linear

The linear subset is comprised of fold patterns containing a linear backbone extending from one end of the chain to the other. A typical crease pattern for this subset is given in Figure 2.14(a). The actuation of the chain is accomplished by applying forces on opposing panels in the chain such that a moment about the backbone is created. This input force triggers either an extension or contraction of the chain along the chain's backbone depending on the direction of the applied moment. This output motion is demonstrated in Figure 2.15. While this motion is back-drivable it can become impractical as the extension of the chain can often be several times longer than the movement required at the input to create it, thus requiring a greater stroke length or a larger number of actuators to back-drive.

When actuating models from this subset the direction of the branching folds from the chain and their angle relative to the backbone will dictate the maximum distance of the extension along the backbone. As the angle between the branching folds and the backbone decreases the distance of the extension goes to a minimum while the closer the angle comes to 90° the greater the extension.

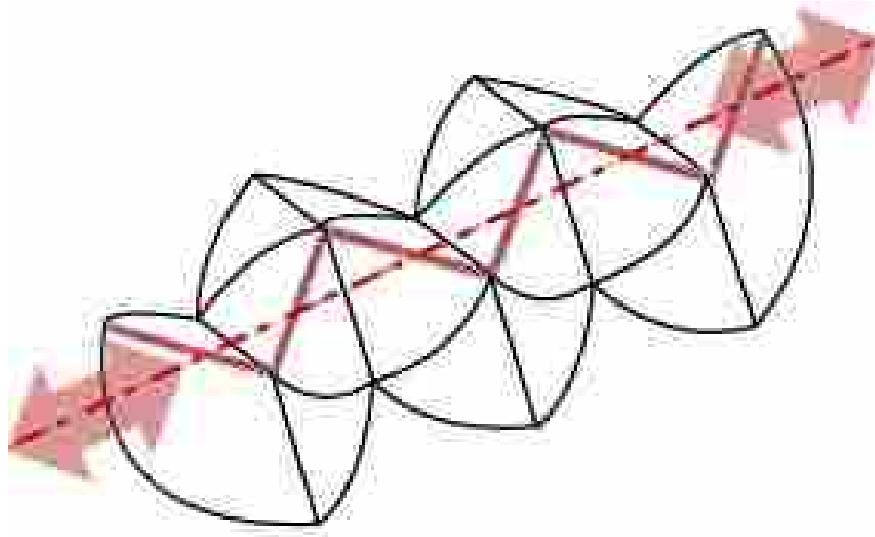


Figure 2.16: A fold pattern belonging to Subset LC2 showing the kinked backbone (solid red), linear pseudo-backbone (dashed-red), and extension/contraction output motion (red arrows).

At an angle of 90° there is no extension of the chain – just a hinge-like folding of the chain about the backbone.

While fold patterns in this subset are kinematically 1 DOF systems, when actuating models folded from paper (or other low-stiffness materials) not all the panels in the fold pattern will be involved in the output motion. As the compliance of the material being used to create the mechanism increases the extension motion of the chain will only move forward along the chain originating from the point of actuation. This means that if the actuation force is applied near the middle of the chain, folds and panels before this point will not be actuated as a result of this force. Therefore, to ensure actuation of all panels in such models, the input forces should be applied at the root of the chain.

Subset LC2 - Kinked

The kinked subset of the N-Long Linear Chain class is similar to the linear subset in that both subsets exhibit an extension or contraction along a linear backbone as shown in Figure 2.16. In the case of the kinked subset this extension occurs along an imaginary “pseudo-backbone” shown in the crease pattern given in Figure 2.14(b). This motion is initiated by a moment applied about

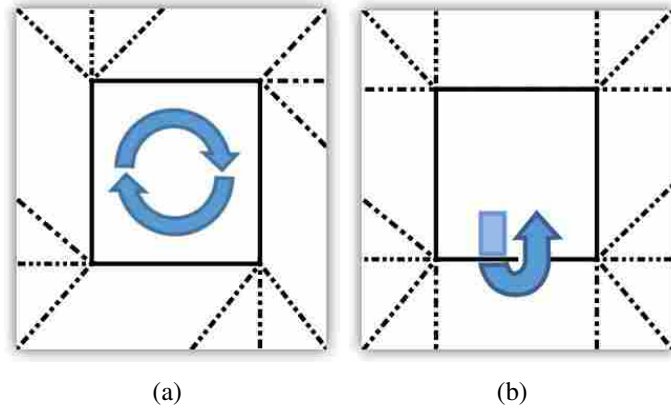


Figure 2.17: Crease patterns belonging to Subsets SL1 (a) and SL2 (b) showing the direction of the center loop’s rotation.

the backbone. The kinked subset differs from Subset LC1 because, due to the kinked nature of the backbone, the extension of the chain will always occur in both directions along the pseudo-backbone from the point of application of the input forces. Also, depending on the compliance of the panels of the material, the fold pattern can exhibit a curving of the chain. This motion is achieved by warping the panels of the fold along the length of the chain and thus violates rigid-foldability constraints. However, in some applications this secondary motion could be desirable. For instance, in the origami model “Scary Snake” [15] the curving of the chain is used to create a chomping type of motion. Another example would be “Randlett’s Bird” [13] which uses the curving of the chain to cause the wings of the bird to flap. The curvature created in the chain is increased by decreasing the distance between kinks in the backbone of the chain. Like Subset LC1 this subset may be impractical to back-drive because the output displacement is much greater than the the input.

2.4.4 Single Loop Network

Up to this point, the fold patterns discussed have all been open chains. However, some discussion of a closed network should be included in our investigation of fundamental motions in origami designs. A network is defined as a set of linked spherical mechanisms that create a closed loop such that there is no distinct beginning or end. In origami designs there are networks of great complexity with very unique movements. However, a fundamental network to consider

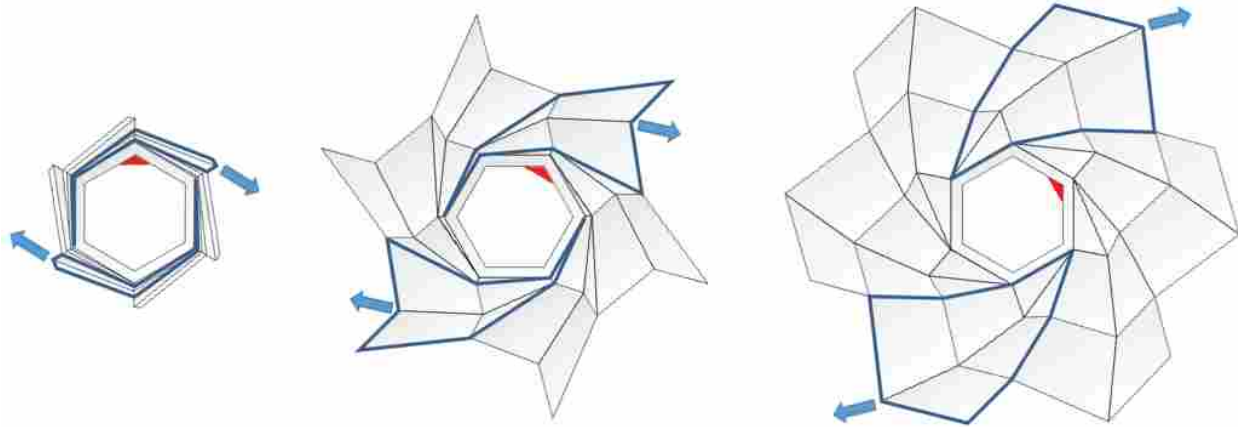


Figure 2.18: A hexagonal flasher belonging to Subset SL1 showing in-plane rotation of the central loop and radial expansion motions of the flasher as well as the direction and location of the forces that create them (blue arrows).

is that of the Single Loop outlined by Bowen et al. [8] and discussed earlier in this chapter. This class contains two subsets - SL1 and SL2. Generic crease patterns typical of each subset are shown in Figure 2.17. Origami models in two subsets for this class are distinguished from each other by the direction the center loop rotates once the model is actuated: either in the ground plane (Subset SL1) or out-of-plane (Subset SL2) as demonstrated in the figure. While these crease patterns show a square center loop there is no requirement that the loop be square.

Subset SL1

This subset of the Single Loop class generally consists of the various origami flasher designs. While many flashers are not rigidly foldable their crease patterns can be easily altered to allow for rigid-foldability constraints. A general crease pattern belonging to the SL1 subset is given in Figure 2.17(a), which also shows the characteristic in-plane rotation of the center loop. The specific motion of fold patterns belonging to Subset SL1 as well as the actuation to create it can be rather complicated. Figure 2.18 shows three stages in the motion of a hexagonal flasher starting at a fully stowed position and moving to a fully deployed (flat) state. The motion is created as forces are applied to opposing sides of the flasher (highlighted in blue in the figure). As these forces are applied the fold pattern will unfold and expand radially until finally reaching the final flat state. Notice also how the inner loop rotates in the ground plane as the fold pattern is actuated. In some

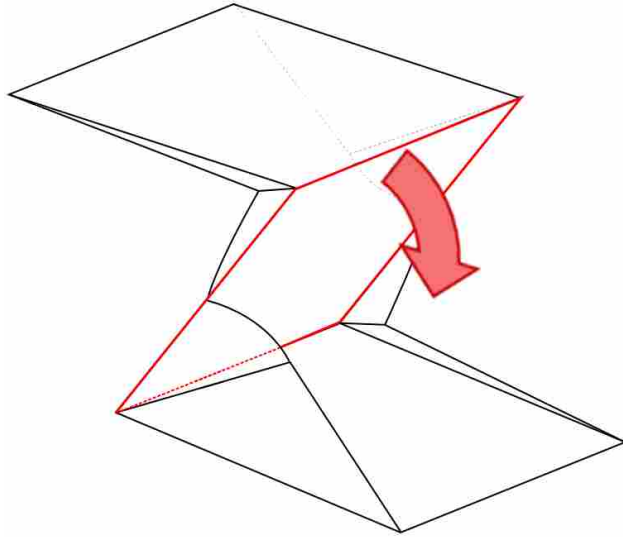


Figure 2.19: Output motion (red arrow) of Subset SL2 showing the out-of-plane rotation of the center loop (outlined in red).

applications applying actuation forces to the outer edges could be undesirable or infeasible. In this case, another possible actuation technique could be to rotate the center causing radial expansion due to centrifugal force. This second actuation technique may present a new set of limitations as a mechanism could require a prohibitively high force to create the rotation of the center loop. Fold patterns belonging to this subset have multiple DOF's and are therefore not back-drivable.

Subset SL2. Origami fold patterns belonging to this subset typically have crease patterns similar to Figure 2.17(b) and exhibit a hinge-like rotation of the center loop out of the ground plane (as shown in Figure 2.19). This motion is created by applying a moment about the hinge of rotation. The location of this hinge is determined by the folds branching off from the loop. For instance, considering the crease pattern from Figure 2.17(b), either the top or bottom of the square loop could be a potential hinge because none of the branch-offs intersect the space directly above or below those fold lines. The hinges will always lie on one of the edges of the center loop. Like Subset SL1, this subset is not back-drivable.

2.5 Results

From the 140 models analyzed in this study, 11 distinct types of motion were identified and defined. Subsets inside an existing classification framework were created. This extension of the classification scheme first proposed by Bowen et al. [8] allows for increased understanding of the network of spherical mechanisms causing the motion and the types of motions exhibited by origami models themselves. Table 2.1 gives a summary of these findings.






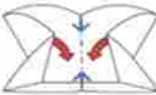



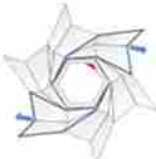

2.6 Conclusion

This chapter presented the results of an in-depth study of kinematic action origami models and defined fundamental motions. The information provided will serve to create a better understanding of the fundamentals of actuating origami-inspired mechanisms. This is an important step in advancing origami-compatible actuation technology as well as in the development of complex, fully actuated, origami-inspired mechanisms.

While this chapter has established a basic understanding of some fundamental motions in origami models and how to actuate them, further study is required to establish a more rigorous understanding of their kinematics. Such studies may involve investigating the mechanical advantage, energy storage, or other performance characteristics of each of the classes. Further study could also explore the characteristics of more complex origami models including how the subsets discussed here combine their motions in these more complicated designs.

As kinematic rigor is applied to defining and predicting the movements of origami models, the mechanisms that they inspire will be able to grow in complexity and specialization. Customized origami-compatible actuation systems will begin to be developed to create fully actuated origami-based mechanisms. As a result origami inspired mechanisms will be able to find more wide-spread application in solving challenging and otherwise impossible engineering problems.

Table 2.1: Summary of characteristic motions and actuation inputs for each subset.

Subset	Actuation Force Type	Actuation Force Location	Rigidly Foldable	Back-Drivable	Output Motion
S1a	Forces or Moment	<u>Forces</u> : External flaps <u>Moment</u> : Backbone	Yes	Yes	
S1b	Out of Plane Force	Panels with sector angle less than 90 deg.	No	No	
S2	Forces	External flaps on center panels	Yes	No	
S3	In-Plane Force (sliders) or Out-of-Plane Point Force	<u>Sliders</u> : Along mountain folds <u>Point Force</u> : Fold vertex	Yes	No	
C1	Forces or Moment	<u>Forces</u> : External flaps <u>Moment</u> : Backbone between driving panels	Yes	Yes	
C2	Forces or Moment	<u>Forces</u> : External flaps <u>Moment</u> : Backbone between driving panels	Yes	Yes - creates a linear extension	
C3	Forces or Moment	<u>Forces</u> : External flaps <u>Moment</u> : Backbone between driving panels	Yes	Yes - creates a parallel-guided mechanism	
LC1	Forces or Moment	<u>Forces</u> : External flaps <u>Moment</u> : Backbone between driving panels	Yes	Difficult - increased stroke and/or number of actuators required	
LC2	Moment	Backbone between driving panels	Yes - compliant panels allow for curving of the backbone	Difficult - increased stroke and/or number of actuators required	
SL1	Forces or In Plane Rotation	<u>Forces</u> : Opposing corners of center loop <u>In Plane Rotation</u> : Center loop causing rest of fold pattern to move	Yes - modification of crease patterns may be needed	No	
SL2	Moment	One of the fold lines defining the edges of center loop	Yes	No	

CHAPTER 3. CONSIDERING MECHANICAL ADVANTAGE IN THE DESIGN OF ORIGAMI-BASED MECHANISMS

3.1 Introduction

Origami-based mechanisms offer the potential for unique solutions to engineering problems. As increased rigor is brought to the engineering study of origami, the number of possible applications of these mechanisms promises to grow. Already origami-based designs can be seen in the medical field [2, 17], aerospace [4], aircraft construction [3, 18], batteries [19], and robotics [20–22]. While the use of origami-based mechanisms can be attractive to designers, the design process is non-trivial and an understanding of key design parameters will assist in fully realizing the benefits of origami-based mechanisms. This is particularly important when the mechanism being designed is required to perform a mechanical task and it is essential to meet required performance characteristics such as force-deflection behavior and mechanical output.

The study of mechanical advantage – the ratio of mechanical force output to driving input – can yield useful insight into the behavior of a mechanism. Mechanisms with greater mechanical advantage allow a greater output force to be achieved from a given input. The study of mechanical advantage can also give insight into relative velocities as well as displacements between the output and input of a mechanism. For some applications a low mechanical advantage may be desirable, in order to increase the output to input displacement ratio (geometric advantage [23]). Increasing the geometric advantage of a mechanism is particularly useful when looking to develop actuators/mechanisms with greater stroke. Since mechanical advantage is so closely tied to force outputs, actuation, and displacements it can be helpful when seeking to better understand the parameters controlling the performance of a mechanism.

The objective of this chapter is to demonstrate the effect of design decisions on the performance of origami-based mechanisms. This is done by developing a mechanical advantage model and exploring the effects of key parameters within the model as well as how they affect the funda-



Figure 3.1: Origami vertex (shown in grey) with an equivalent rigid-body spherical mechanism and the axes of its revolute joints (shown in blue).

mental design decisions of surrogate hinge selection, actuation input, and fold pattern modification. Each parameter is studied within the scope of the model, then their effect on the design of origami-based mechanisms is discussed. Included in this final discussion are practical considerations to be made during the design process relating to each key parameter.

3.2 Background

Origami has existed as an art form for thousands of years and origami artists have developed a vast number of models with various levels of complexity. However, when seeking inspiration for mechanisms a specific subset of origami – kinematic action origami – is particularly attractive as it is characterized by models that exhibit motions in their folded state that can be predicted and analyzed using conventional kinematics.

Kinematic action origami models can be modeled as spherical mechanisms [9–12, 24] where each vertex is represented as a spherical center, the panels as rigid links, and fold lines as revolute joints. An example of this is shown in Figure 3.1, where the origami vertex is shown (in grey) with an equivalent rigid-body spherical mechanism super-imposed (shown in blue). This kinematic representation of origami models is made possible due to rigid foldability assumptions, which state that all motion in the origami model comes from folding localized about crease lines

(such that there is no deflection in the panels). Origami models for which this assumption is appropriate are described as “rigidly foldable”.

Using this representation of origami models has allowed work to be done studying and further classifying models within this set of origami. Bowen et al. [8] created a classification system that grouped kinematic action origami models based on the spatial relationships between the vertices of their associated fold pattern. From this classification scheme the fundamental movements of origami models were studied and classified into subsets exhibiting similar types of motion [1].

To advance the work being done to understand and predict the behaviors of origami-based mechanisms, this chapter will provide models and methods to evaluate the effects of design choices on their performance – allowing designers to ensure that the final product will meet required functional characteristics.

3.3 Mechanical Advantage Model

This section presents models for mechanical advantage in origami-based mechanisms consisting of degree-4 vertices. Discussion of the model will first focus on a single origami vertex followed by modelling origami patterns with N linearly-linked vertices.

3.3.1 Modelling a Single Origami Vertex

A general degree-4 vertex is shown in Figure 3.2. The sector angles (spherical link lengths) are indicated by α while the dihedral angles (angles between panels) are indicated by θ . Note that θ_n gives the angle between panels α_n and α_{n+1} . An assumption inherent in the following discussion is that the fold pattern being considered is rigidly foldable. Further, in order to maintain a 1 DOF system, only fold assignments that create fully coupled motion (all panels move at the same time) are considered. For example, the vertex shown in Figure 3.2 has the fold assignment of three valleys and one mountain - where the mountain fold is θ_3 . While there are other fold assignments that meet rigid foldability requirements, they rely on sequential folding - thus making the vertex a 2 DOF system. Lastly, the vertices considered in this model have opposing fold assignment between θ_1 and θ_3 (i.e. if the θ_1 fold line is a valley then the θ_3 fold line is a mountain).

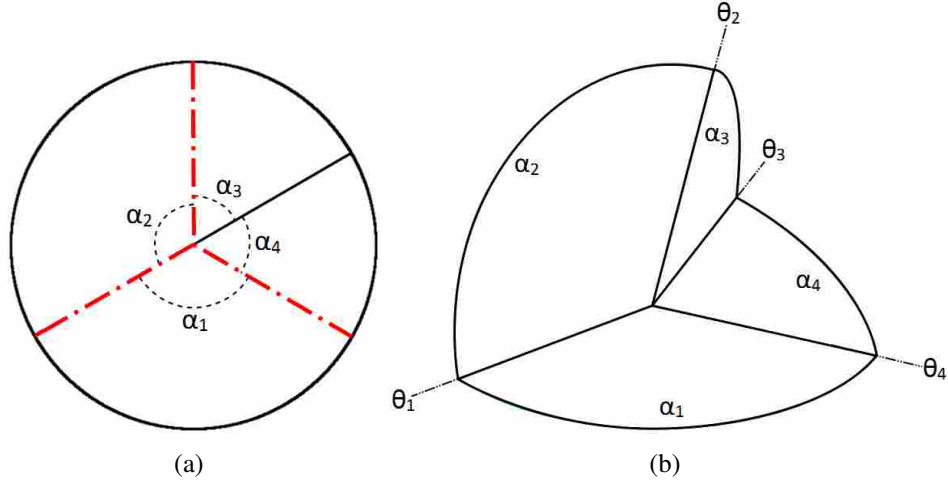


Figure 3.2: General degree-4 vertex in flat (a) and folded (b) states with sector and dihedral angles labeled with α and θ respectively. Fold assignments are indicated in (a) with dashed red (valley) and solid black (mountain).

The mechanical advantage for a rigidly foldable, degree-4 vertex with fully coupled motion is:

$$MA = \frac{d\gamma_1}{d\gamma_4} \quad (3.1)$$

where γ is the exterior dihedral angle of panels α_n and α_{n+1} such that

$$\gamma_i = \pi - \theta_i \quad (3.2)$$

Lang [25] showed that the mechanical advantage can be written explicitly (in terms of the driving angle γ_1), as:

$$MA = \frac{\mu^2 \tan^2(\frac{\gamma_1}{2}) + 1}{\mu [\tan^2(\frac{\gamma_1}{2}) + 1]} \quad (3.3)$$

where μ was defined as

$$\mu = \frac{\sin(\frac{1}{2}(\alpha_3 + \alpha_2))}{\sin(\frac{1}{2}(\alpha_3 - \alpha_2))} \quad (3.4)$$

Using Equation 3.2, one can rewrite Equation 3.3 in terms of θ_1

$$MA = \frac{\mu^2 \cot^2(\frac{\theta_1}{2}) + 1}{\mu [\cot^2(\frac{\theta_1}{2}) + 1]} \quad (3.5)$$

which gives the mechanical advantage of the origami vertex as a function of the interior dihedral angle, θ_1 .

In addition to rigid-foldability, Equations 3.4 and 3.5 assume that the origami vertex is flat-foldable. For a degree-4 vertex, flat-foldability requires that the sector angles for each panel satisfy the following equation:

$$\alpha_1 + \alpha_3 = \alpha_2 + \alpha_4 = \pi \quad (3.6)$$

While there exist closed-form equations for the behavior of rigid, non-flat-foldable, degree-4 vertices they are significantly more complex [26].

Using Equations 3.4 and 3.5, the mechanical advantage of a rigid, flat-foldable, degree-4 vertex can be calculated. However, these equations are unable to account for any stiffness in the hinges of the mechanism. When compliant hinges are introduced into a mechanism the mechanical advantage profiles will be altered [27]. This is due to the fact that each compliant segment acts like a torsional spring resisting the movement of the mechanism, effectively lowering the overall mechanical advantage.

Salamon et al. [27] showed that the mechanical advantage of a mechanism with compliant hinges (MA_c) is of the form:

$$MA_c = MA_r \left(1 - \frac{f_c}{f_{in}} \right) \quad (3.7)$$

where MA_r is the mechanical advantage of an equivalent rigid-body mechanism, f_c is the total force required to deflect all the compliant segments of the mechanism, and f_{in} is the input force. The solution for mechanical advantage of an origami vertex can be found, using virtual work calculations, to be

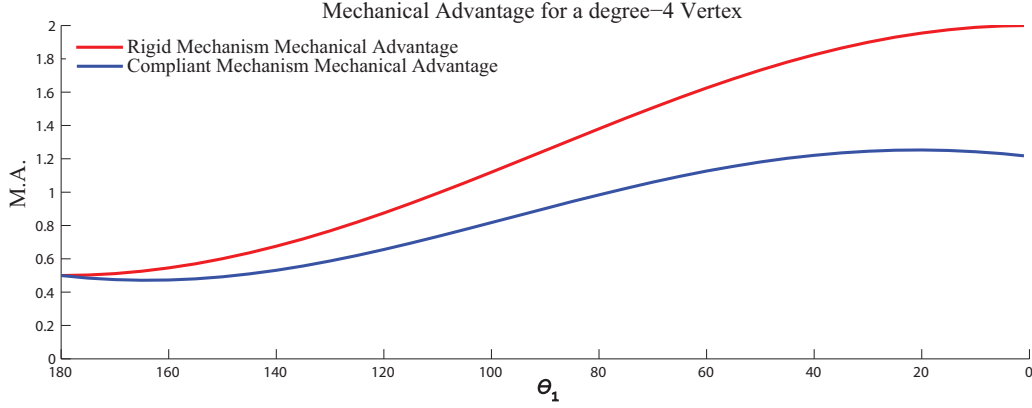


Figure 3.3: MA_r vs. MA_c for a degree-4 vertex with sector angles $\alpha_1 = \frac{2\pi}{3}$, $\alpha_2 = \frac{2\pi}{3}$, $\alpha_3 = \frac{\pi}{3}$, and $\alpha_4 = \frac{\pi}{3}$. The MA_c curve is calculated with $M_{in} = 0.113$ Nm and $k = 0.178$ Nm/radian.

$$\begin{aligned}
 MA_c = MA_r - \frac{MA_r}{M_{in}} & \left[k_1(\theta_{1o} - \theta_1) + k_3(\theta_{3o} - \theta_3) \frac{d\theta_3}{d\theta_1} \right] \\
 - \frac{MA_r}{M_{in}} & \left[k_2(\theta_{2o} - \theta_2) \frac{d\theta_2}{d\theta_1} + k_4(\theta_{4o} - \theta_4) \frac{d\theta_4}{d\theta_1} \right]
 \end{aligned} \tag{3.8}$$

which can be simplified to the form of Equation 3.7

$$MA_c = MA_r \left(1 - \frac{M_c}{M_{in}} \right) \tag{3.9}$$

where

$$M_c = \sum_{i=1}^4 k_i(\theta_{io} - \theta_i) \frac{d\theta_i}{d\theta_1} \tag{3.10}$$

Equations 3.9 and 3.10, used with Equations 3.4 and 3.5, can be used to model the mechanical advantage of a rigid, flat-foldable, origami-based mechanism consisting of a single degree-4 vertex with compliant hinges.

Figure 3.3 demonstrates the difference in the mechanical advantage of a compliant degree-4 vertex and its rigid-body equivalent. Here $\alpha_1 = \frac{2\pi}{3}$, $\alpha_2 = \frac{2\pi}{3}$, $\alpha_3 = \frac{\pi}{3}$, and $\alpha_4 = \frac{\pi}{3}$. Further, all hinges are modelled with identical torsional stiffness of $k = 0.178$ Nm/radian and the motion

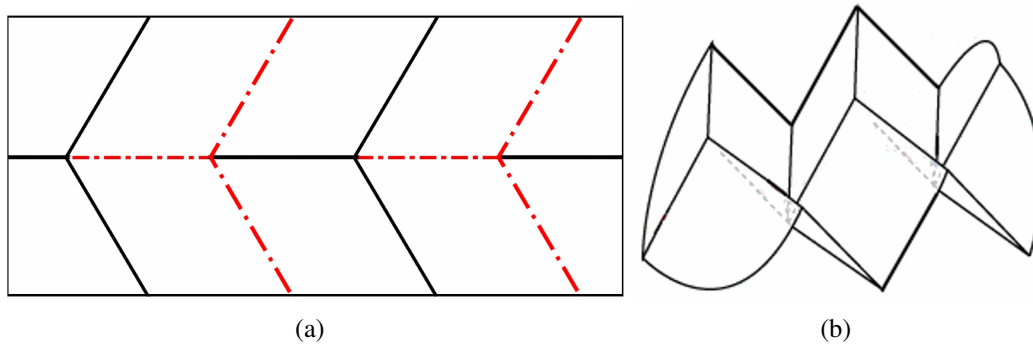


Figure 3.4: Example of a linear-linked origami fold pattern shown both flat (a) and partially folded (b). Fold assignments are indicated in (a) with dashed red (valley) and solid black (mountain).

is driven by an input moment (M_{in}) of 0.113 Nm. The origami vertex begins in a flat position ($\theta_1 = 180^\circ$) and moves until fully folded ($\theta_1 = 0^\circ$). As can be seen from Figure 3.3, including considerations for the compliant hinges decreases the mechanical advantage of the mechanism. Further exploration of the parameters affecting the actuation, force-deflection behavior, and mechanical advantage of origami-based mechanisms is given in Section 3.3.3.

3.3.2 N Linearly-Linked Vertices

Thus far, discussion of the model has focused on a single degree-4 vertex. In this section, equations for the mechanical advantage of origami-based mechanisms with N linearly-linked, degree-4 vertices are developed. Here linearly-linked means that each vertex is linked to neighboring vertices in the fold pattern such that the fold line associated with θ_3 of a given vertex is coupled directly to the input (θ_1) of the adjacent vertex and the two fold lines are *collinear*. Additionally, each vertex in the fold pattern has alternating fold assignments such that one vertex has three mountain folds and one valley, while the subsequent vertex has three valleys and one mountain. Finally, the constraint of fully coupled motion imposed in the previous section is again enforced - so that fold assignments that create sequential folding are not considered (i.e. the chain is 1 DOF).

An example of linearly-linked vertices with alternating fold assignments is given in Figure 3.4. It should be noted that there are numerous ways of linking origami vertices into a chain-type fold pattern (each with their own mechanical advantage behaviors); however, in order to better

demonstrate the fundamental parameters affecting the performance of origami-based mechanisms the simplest, most symmetric scenario was chosen.

The mechanical advantage of a linearly-linked chain of origami vertices is

$$MA = \frac{d\theta_{in}}{d\theta_{out}} \quad (3.11)$$

where θ_{in} is the input of the first vertex while θ_{out} is the output (θ_4) of the last vertex in the chain. A connection between these two angles is established using the relation of θ_1 and θ_3 in a degree-4, flat folding, rigidly foldable, origami vertex given by Hull [28] which is:

$$\theta_1 = -\theta_3 \quad (3.12)$$

Two degree-4 vertices that are linearly-linked will be coupled such that the input angle of the second vertex (θ_{1_2}) is equal to θ_3 of the first vertex (θ_{3_1}). Given Equation 3.12 and this coupling of vertices in the chain, one can see that $\theta_{1_1} = -\theta_{1_2}$. Thus for N linearly-linked vertices the relationship between θ_{1_1} and θ_{1_n} is:

$$\theta_{1_1} = (-1)^{n-1} \theta_{1_n} \quad (3.13)$$

where n is the number of vertices in the fold pattern. With this relationship established, the rigid-body equivalent mechanical advantage is found using:

$$MA = \frac{d\theta_{1_1}}{d\theta_{4_n}} = [(-1)^{n-1}] \frac{d\theta_{1_n}}{d\theta_{4_n}} \quad (3.14)$$

which becomes:

$$MA = [(-1)^{n-1}] \frac{\mu_n^2 \cot^2\left(\frac{\theta_{1_n}}{2}\right) + 1}{\mu_n [\cot^2\left(\frac{\theta_{1_n}}{2}\right) + 1]} \quad (3.15)$$

where μ_n is calculated with Equation 3.4 using the sector angles associated with the n^{th} vertex of the mechanism.

Equation 3.15 gives an interesting insight into the mechanical advantage of a chain of linearly-linked, flat-foldable, degree-4, vertices. While not immediately obvious, it can be seen

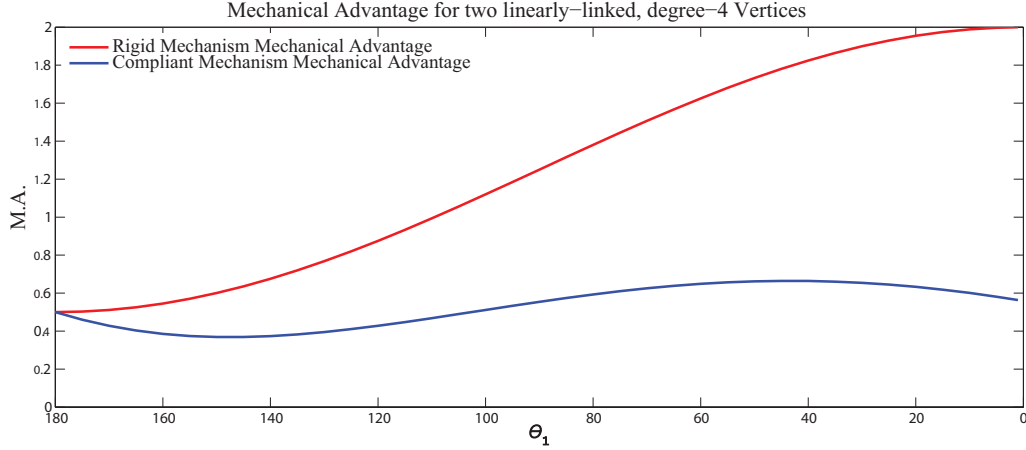


Figure 3.5: MA_r vs. MA_c for a mechanism consisting of two, linearly-linked, degree-4 vertices with sector angles $\alpha_1 = \frac{2\pi}{3}$, $\alpha_2 = \frac{2\pi}{3}$, $\alpha_3 = \frac{\pi}{3}$, and $\alpha_4 = \frac{\pi}{3}$. The MA_c curve is calculated with $M_{in} = 0.113$ Nm and $k = 0.178$ Nm/radian.

that the rigid-body equivalent mechanical advantage is entirely determined by the final vertex in the chain. This is because, due to the constraints of linearly-linked chains defined earlier, the magnitude of the mechanical advantage of the first to $(n - 1)^{th}$ vertices are constrained to be 1. This means that the sector angles for these vertices can be modified as desired (as long as they remain flat-foldable) to capture the desired motion without affecting the mechanical advantage. This gives designers great freedom in creating mechanisms with desired motions without having to compromise mechanical advantage. This is only true, however, for the rigid-body equivalent as the hinge stiffnesses in each vertex will affect the overall mechanical advantage.

To include considerations for compliant hinges in the mechanism, Equation 3.15 must be modified. Recalling the form of Equation 3.9, which gives the mechanical advantage for a single vertex, the mechanical advantage of N linearly-linked vertices is:

$$MA_c = \prod_{j=1}^{n-1} \left[\left(-1 + \frac{M_{c_j}}{M_{in}} \right) \right] \left[MA_{r_n} \left(1 - \frac{M_{c_n}}{M_{in}} \right) \right] \quad (3.16)$$

where

$$M_{c_j} = \sum_{i=1}^4 k_{i_j} (\theta_{i_{o_j}} - \theta_{i_j}) \frac{d\theta_{i_j}}{d\theta_{1_j}} \quad (3.17)$$

Using Equations 3.16 and 3.17, the mechanical advantage for a system of N linearly-linked, degree-4 vertices can be calculated. Figure 3.5 shows a mechanical advantage plot (both the rigid-body equivalent and that for a mechanism with hinge stiffnesses of 0.178 Nm/radian) for a fold pattern consisting of two, linearly-linked, degree-4 vertices driven by an input moment of 0.113 Nm. Both vertices consist of sector angles given by: $\alpha_1 = \frac{2\pi}{3}$, $\alpha_2 = \frac{2\pi}{3}$, $\alpha_3 = \frac{\pi}{3}$, and $\alpha_4 = \frac{\pi}{3}$.

3.3.3 Key Parameters Affecting Mechanical Advantage

Recalling Equations 3.4, 3.5, 3.9, and 3.10, the parameters affecting mechanical advantage are:

M_{in} : input moment driving the motion of the mechanism

k : torsional stiffness of the hinge about the fold axis

α : sector angles of the panels

θ_{i_o} : initial position of the vertex panels

Since origami-based mechanisms are generally manufactured from a flat sheet, the value of θ_{i_o} for many cases will be 180° . Therefore, the remaining discussion will focus on the effects of the other parameters listed: hinge stiffness, input actuation moment, and fold pattern sector angles.

Hinge Stiffness

When using compliant hinges in an origami-based design, each hinge can be modeled as a torsional spring with an associated k-value. Modifying the hinges to change their torsional stiffness can significantly affect on the mechanical advantage of the mechanism. This is demonstrated in Figure 3.6, which shows several mechanical advantage profiles for the vertex already considered ($\alpha_1 = \frac{2\pi}{3}$, $\alpha_2 = \frac{2\pi}{3}$, $\alpha_3 = \frac{\pi}{3}$, and $\alpha_4 = \frac{\pi}{3}$) with input moment $M_{in} = 0.113$ Nm.

An interesting phenomenon is shown in Figure 3.6 when $k = 0.890$ Nm/radian. The plot shows that the mechanical advantage crosses the x-axis and becomes negative. This behavior can

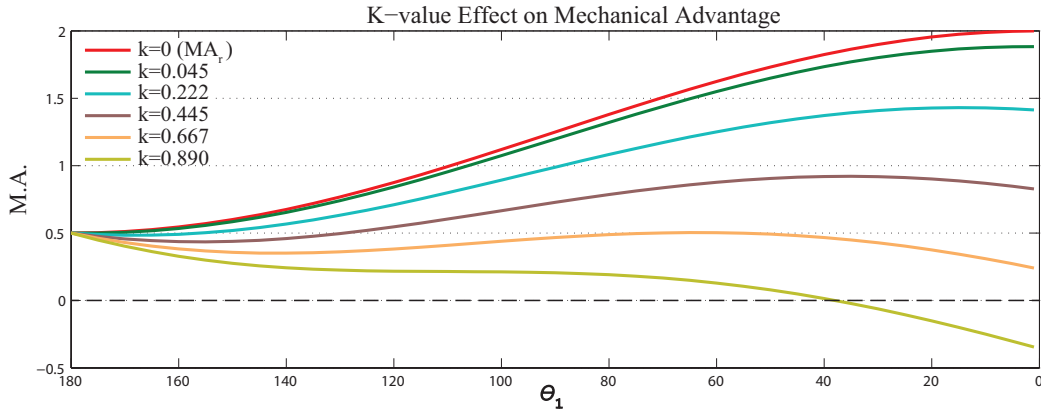


Figure 3.6: Effect of compliant hinge stiffness (k) on mechanical advantage of a degree-4 vertex with $M_{in} = 0.113$ Nm.

be explained by recalling Equation 3.9, which shows that the mechanical advantage is equal to the rigid-body mechanical advantage multiplied by the quantity: $(1 - M_c/M_{in})$. If M_c is ever greater than M_{in} the result will be a negative value. This negative result indicates that the total moment necessary to flex the compliant segments is greater than the input moment. In the plot shown in Figure 3.6 for $k = 0.890$ Nm/radian the mechanical advantage crosses the x-axis at roughly $\theta_1 = 40^\circ$, this means that in order to move beyond $\theta_1 = 40^\circ$ and achieve the desired range of motion (ROM), the hinge stiffness would need to be decreased. In this way, calculation of the mechanical advantage can be used to predict the hinge stiffness needed to achieve a certain ROM with a given input force.

Input Actuation Moment

When designing a mechanism the actuation moment is often initially unknown. In such cases it can be useful to predict the minimum actuation moment required for the mechanism to achieve a given deflection. Again, recalling Equation 3.9, the minimum actuation moment can be determined by setting M_{in} equal to M_c for a desired deflection of θ_1 . Explicitly, for a single degree-4 vertex being actuated to a given driving angle, θ_1 , the minimum input moment required to achieve the motion is:

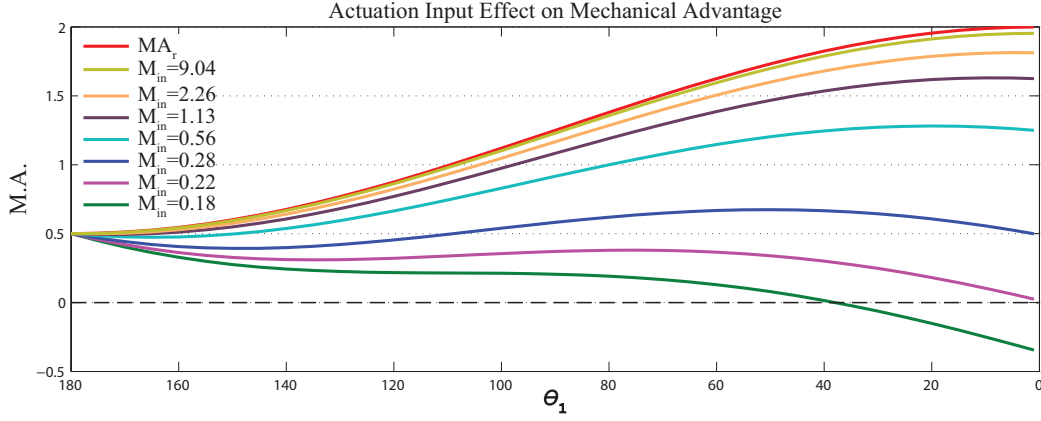


Figure 3.7: Effect of input force (M_{in}) on mechanical advantage of a degree-4 vertex where $k = 0.890$ Nm/radian.

$$\begin{aligned}
 M_{in} = k_1(\theta_1 - \theta_{1o}) + k_2(\theta_2 - \theta_{2o}) & \left[\frac{\mu(\cot^2(\frac{\theta_1}{2}) + 1)}{\mu^2 \cot^2(\frac{\theta_1}{2}) + 1} \right] \\
 -k_3(\theta_3 - \theta_{3o}) + k_4(\theta_4 - \theta_{4o}) & \left[\frac{\mu(\cot^2(\frac{\theta_1}{2}) + 1)}{\mu^2 \cot^2(\frac{\theta_1}{2}) + 1} \right]
 \end{aligned} \tag{3.18}$$

where the interior dihedral angles, θ_2 , θ_3 , and θ_4 are found with the following relationships given by Lang [25]:

$$\theta_2 = \pi - 2 \tan^{-1} \left[\mu \tan \left(\frac{\pi - \theta_1}{2} \right) \right] \tag{3.19}$$

$$\theta_3 = -\theta_1 \tag{3.20}$$

$$\theta_4 = \theta_2 \tag{3.21}$$

and μ is found using Equation 3.4.

Figure 3.7 shows the effect of the input moment (M_{in}) on the mechanical advantage of the vertex considered in the previous plots with hinge stiffness of $k = 0.890$ Nm/radian. As can be seen from Figure 3.7, a minimum input moment of $M_{in} = 0.22$ Nm is required to obtain the full 180° ROM. However, the MA at the end of the ROM is shown to be 0 – meaning the mechanism could

only achieve the motion if unloaded. For there to be any output from the mechanism the actuation moment would need to be greater. This is an interesting result of introducing compliant hinges into a mechanism – the possibility of having a scenario where all the actuation input is absorbed into the strain energy of the deflecting hinges, leaving nothing to achieve any mechanical task. The ability to predict the minimum actuation moment allows designers to discover if the mechanism being developed could even be actuated given the abilities of the available actuators.

In applications where the magnitude of the driving moment is large in relation to the stiffness of the compliant hinges (at least 10^n times greater – where n is the number of vertices in the fold pattern) the mechanical advantage of the compliant mechanism will closely approximate that of its rigid-body equivalent. This can be seen from Figure 3.7 as the mechanical advantage plot of the origami vertex associated with an input moment of 9.04 Nm (roughly 10 times greater than the k -value of 0.890) closely approximates the equivalent rigid-body mechanical advantage plot (MA_r).

Finally, when dealing with large chains of linearly-linked vertices, it may become necessary to use multiple inputs. The position of these inputs in the chain can be found using the calculations for the minimum actuation moment discussed earlier. This is done by finding the mechanical advantage of a chain of linked vertices. As the number of vertices in the chain increases, so will the value for M_c . When the value for M_c becomes greater than or equal to that for M_{in} (after the addition of the i^{th} vertex), the chain will no longer be able to fully actuate. If modification of the hinges or actuation input is not desired then a second actuation input can be added at the input to the i^{th} vertex.

Fold Pattern Sector Angles

Modifications of a vertex's sector angles can have a significant effect on its mechanical advantage. However, modifying the sector angles of a vertex can also affect its motion. Additionally, when modifying the fold angles one must be careful that flat and rigid foldability requirements are still met. Figure 3.8 shows the effect of sector angle modification on the mechanical advantage of a vertex with compliant hinge stiffnesses $k = 0.222$ Nm/radian and an input moment $M_{in} = 0.113$ Nm. The mechanical advantage plot is shown as α_2 ranges from $\frac{11\pi}{18}$ (110°) to $\frac{13\pi}{18}$ (130°) with a

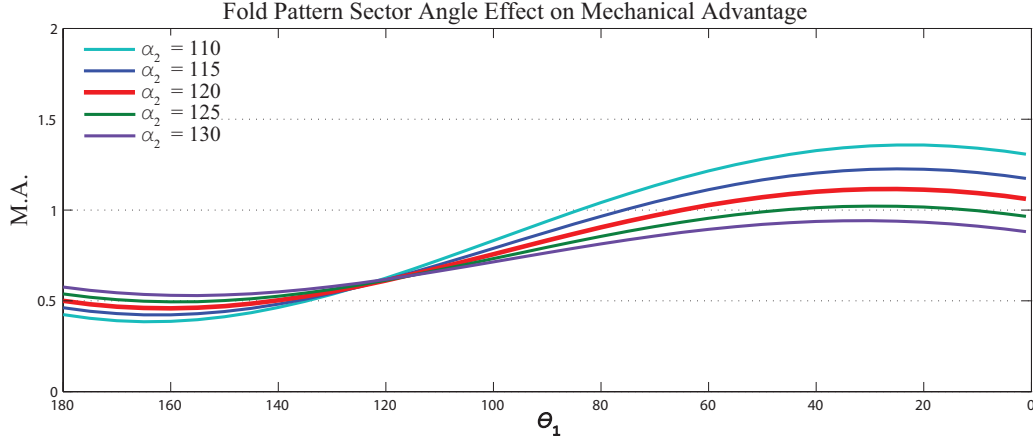


Figure 3.8: Effect of the sector angles (α) in a degree-4 origami vertex on mechanical advantage. Here α_2 is modified from its nominal value of $\frac{2\pi}{3}$ (red). Hinge stiffness and actuation input are: 0.222 Nm/radian and 0.113 Nm respectively.

nominal value (shown in red) of $\frac{2\pi}{3}$ (120°). As the sector angles in a degree-4 vertex approach $\frac{\pi}{2}$ the mechanical advantage increases.

In Figure 3.8, only α_2 was modified (and correspondingly α_4 to maintain the relationship given in Equation 3.6). If all the sector angles are modified simultaneously then the mechanical advantage may be more affected by a given change in the sector angles.

3.4 Key Parameters' Effect on Origami-based Design

With a basic understanding of the key parameters' effect on the mechanical advantage and force-deflection behavior of origami-based mechanisms established, their role in the design of origami-based mechanisms can be explored.

3.4.1 Surrogate Hinges

Origami-based mechanisms derive their motion from the folding of rigid panels about hinges (either revolute or compliant) which act as surrogates for paper folds, and selecting hinges can be one of the most critical design decisions when developing origami-based mechanisms. The hinges being used largely determine the achievable motion of the mechanism and the required actuation force by their stiffness and angular ROM. For this reason it is desirable to use hinges that have low stiffness and large ROM.

Additionally, when using compliant hinges the mechanisms can be further affected by the introduction of secondary parasitic motions. Research has been done on the design of surrogate hinges to improve their ability to model the motion of creased hinges and minimize the introduction of parasitic motions [29–31]. Secondary motions can be reduced by knowing the loading conditions at a fold line and selecting a compliant hinge that will resist the secondary motions associated with those loading conditions. In this way the hinges need not resist all types of secondary motions but only those that will be present under normal conditions. For instance, if compressive and bending loads are known to exist at a hinge then compliant hinge geometries that can resist compression without buckling while still allowing bending should be considered. More information on which types of loads a given compliant hinge is able to resist is given by Delimont et al. [30].

3.4.2 Actuation Inputs

From the discussion of the mechanical advantage of origami-based mechanisms it is clear that actuation inputs have an effect on the final performance. In many cases the limitations of the available actuation technology can determine the design of the mechanisms. For this reason the achievable actuation force, as well as any limitations on stroke length, should be considered early in the design. If the actuation input to an origami-based mechanism is low the result could be reduced ROM or inability to perform mechanical tasks (even cases where there is no force output). Any of these problems would result in a mechanism being unable to function properly. For this reason it is suggested that designers work to find a balance between design parameters, particularly hinge stiffness, such that desired ROM and outputs are achieved without requiring prohibitively high actuation inputs. If the required actuation input becomes too large a possible solution could be the use of multiple inputs. The location of each input can be determined using the Equations 3.18- 3.21 as discussed in Section 3.3.3.

3.4.3 Fold Pattern Sector Angles

The kinematics of a given origami-based mechanism are largely determined by the fold pattern being used. If a specific motion is required from a mechanism this can only be achieved through modification of the sector angles. When dealing with mechanisms consisting of a single

vertex, once this motion has been achieved, only small modifications can be made to the sector angles to fine-tune the mechanical advantage of the mechanism. However, if the mechanism is based on a fold pattern consisting of linearly-linked, flat-foldable, degree-4 vertices designers have much greater freedom to modify the sector angles of the fold pattern. As a result, designers are better able to achieve the desired output motion and kinematics without compromising mechanical advantage and vice versa.

3.5 Conclusion

A model for calculating mechanical advantage in a rigid, flat-foldable origami-based mechanism consisting of N linearly-linked, degree-4 vertices was presented and key parameters affecting the force-deflection behavior and mechanical advantage were discussed. The results enable designers to predict the required actuation force and/or maximum ROM of a fold pattern as well as gain familiarity with the effect of fundamental design decisions on origami-based mechanisms.

In the development of actuated origami-based mechanisms it is important to have a good understanding of the parameters controlling their force-deflection behavior, motion, and mechanical advantage. The mechanical advantage model and parameters developed in this chapter will allow designers to gain this critical understanding and better see the effect of certain design decisions on the functionality and actuation of the final mechanism. This may enable designs with more complexity and functionality.

In conventional design problems, years of experience and study have created guidelines and tools that designers can use to accurately model and analyze the behavior of their design. The topics discussed in this chapter are a step towards such an understanding of origami-based mechanisms.

As designers of origami-based mechanisms become aware of more design considerations specific to origami-based design, their ability to fully realize the potential benefits of origami-based mechanisms will increase.

CHAPTER 4. CONSIDERATIONS FOR THE SELECTION OF SURROGATE HINGES IN ORIGAMI-BASED MECHANISMS

4.1 Introduction

The use of origami-based mechanisms as solutions to engineering problems has become an area of great interest for designers. Origami-based mechanisms have unique motions [1], allow for simpler manufacturing methods [32–34], are highly storable [2, 35], and have the ability to be reconfigurable [7, 36, 37]. With this unique set of characteristics, origami-based mechanisms are able to offer solutions to engineering challenges in a wide variety of applications. As designers develop greater familiarity with the effective design of origami-based mechanisms the applications of such mechanisms will become even more widespread.

While the use of origami-based mechanisms in engineering applications is attractive, the design process can be difficult and without well-established guidelines designers may find it difficult to fully capture their benefits. The previous chapter presented a detailed study of the parameters affecting the performance of origami-based mechanisms. From this study three parameters – actuation input, fold pattern sector angles, and surrogate hinge stiffness – were shown to have significant effect on the force-deflection and mechanical performance of origami-based mechanisms. Of these three parameters, surrogate hinge stiffness can have a significant effect on performance; due to the fact that the overall precision, range of motion (ROM), and mechanical advantage of the mechanism being developed are largely decided by the hinges being used. This chapter will discuss practical considerations relating to the selection of surrogate hinges for use in origami-based mechanisms.

The objective of this chapter is to give designers a better understanding of considerations to be made in selecting surrogate hinges. The considerations presented here will discuss minimizing the hinge imprint, reducing undesirable motions (such as parasitic motion and reduced ROM), and creating hinges in metals. By giving designers greater insight into a critical parameter control-

ling the performance of origami-based mechanisms, the design of more precise and predictable mechanisms will be facilitated. In turn, designers will be better able to capture the benefits of origami-based mechanisms in applications beyond current limitations and expand to new areas in engineering.

4.2 Background

When looking to develop origami-based mechanism a specific subset of origami – kinematic action origami – can provide useful inspiration, as models belonging to this subset exhibit motions that can be analyzed through conventional kinematics.

Kinematic action origami models are modeled as spherical mechanisms [9–12, 24] with each vertex represented as a spherical center, surrounding panels as rigid links, and fold lines as revolute joints. To account for the compliant hinges commonly used in origami-based mechanisms the revolute hinges can be assumed to have torsional stiffness, k , which is determined by the geometry of the compliant segments in the hinge.

The design of surrogate hinges can be complex and, as discussed earlier, can have a strong effect on the performance of the mechanism. Compliant hinges allow for easier manufacture, reduced assembly, and remove the need for maintenance – which make them desirable for use in origami-based mechanisms – but they can also introduce parasitic motions and reduce overall ROM if not designed correctly. There has been work done to refine the design of these compliant hinges such that these undesirable behaviors are minimized [29–31].

For applications where the surrogate hinges are to be created in metal there are somewhat fewer examples and studies to reference. However, Ferrell et al. [38] developed surrogate hinges where joints with 3D geometries were developed through sheet metal forming operations. Additionally, work has been done creating origami structures in metal [39]. These preliminary studies represent a starting point for designers seeking to use metal surrogate hinges however there is still much more work to be done to effectively use metals in origami-based mechanisms.

This chapter will further develop the study of surrogate hinges, including those in metals, thereby allowing designers to select hinges that will ensure required performance and minimize undesired behaviors.

4.3 Practical Considerations Relating to Surrogate Hinge Selection

For origami-based mechanisms, designers must use hinges (either compliant hinges or revolute) to act as surrogates for the creases in paper models. Work has been done to find ways of creating hinges in non-paper materials that will approximate some of the behaviors of paper crease hinges. In order to create such a hinge it is necessary to create a localized decrease in stiffness about the fold axis such that the surrounding panels are significantly stiffer in comparison to the “hinge” [38].

Several considerations should be made when selecting the type of surrogate hinge to be used. This section will discuss several of these considerations and how each can affect the mechanism.

4.3.1 Surrogate Hinge Imprint

When selecting a surrogate hinge to be used in an origami-based mechanism it is desirable to minimize its overall imprint. The imprint of a hinge is defined to be its dimension orthogonal to the fold axis. Hinges with larger imprints will limit the compactibility of the mechanism. The ideal hinge will be elongated along the fold axis with little to no imprint orthogonal to it (much like a crease in paper models).

With compliant surrogate hinges, the imprint on the mechanism can be reduced by selecting the appropriate type of flexure. For instance, flexures that create deflection through torsion rather than bending will have a smaller imprint. This is due to the fact that torsional flexures are oriented along the length of a fold axis while bending flexures are oriented orthogonal to it. Thus any increase in length (to increase compliance) of a torsional member will not increase the width of the hinge. For this reason it is more desirable to select compliant surrogate hinges with torsional members.

4.3.2 Required ROM of a Hinge

Depending on the motion of the mechanism, different amounts of angular displacement will be required of each hinge. Generally, in origami models the max ROM for a given hinge will be 180° . Not all sections of a fold pattern, however, may require this full range of motion. For

the section of the fold pattern being considered a hinge must be selected that will have the proper ROM. It should be noted that not many surrogate hinges can create a full 180° rotation so this should only be required of a given hinge if absolutely necessary. Also, hinges with higher ROM's may be more likely to introduce parasitic motion into the final mechanism.

4.3.3 Increasing the Precision of a Hinge

The precision required from a hinge is determined by the function of the mechanism. If extremely high precision is required then each surrogate hinge must be made to minimize parasitic motion and maintain a stable axis of rotation. A revolute joint is an example of a hinge that perfectly resists all parasitic motion and has a stable axis of rotation. Most compliant surrogate hinges, while able to approximate this behavior through a small displacement, will eventually shift their axis of rotation as their geometry deforms. Some will not only shift their axis of rotation but will allow parasitic motions to be introduced into the mechanism. To reduce these secondary motions the compliant hinge stiffness can be increased. However, this comes at the cost of greater actuation inputs to the mechanism. For applications where high precision must be maintained through a large ROM only the revolute joint can be used, but with smaller displacements other surrogate hinges may be appropriate.

4.3.4 Types of Loads on the Hinges

Ideally a hinge will allow only bending about the fold axis and resist all other motions. As this ideal won't be realized in all surrogate hinges it is necessary to be aware of which loads a given hinge *must* resist in order for the motion to propagate as needed through the mechanism. Generally the loads along hinges can be predicted for a given mechanism. Once a designer is aware of the loads (tensile, compressive, shear, etc.) at a given hinge they can decide which ones must be resisted and select an appropriate surrogate hinge. For instance, if compressive and bending loads are known to exist at a hinge then surrogate hinges that can resist compression without buckling while still allowing bending should be considered.

4.4 Selection of Surrogate Hinges in Metals

For applications where the mechanism will be exposed to high temperatures, structural loads, or corrosive environments the polymers commonly used in the creation of compliant hinges will not be appropriate. In such cases the material used to fabricate the mechanism will most likely be a metal. Using metal in the design of origami-based mechanisms allows the mechanism to be used in more demanding applications. However, the design of compliant hinges with large deflections in metals can be a challenge - especially hinges that are at the same time 2D and have a reduced imprint (so as to lend themselves to use in origami-based mechanisms). This section will discuss considerations that can be made in the development of such surrogate hinges.

4.4.1 Network Hinges

In order to decrease the overall length of the hinge, a network of flexures may be used [40]. By combining flexures in series and in parallel the stiffness of a hinge can be tailored to allow a given deflection. The benefit of these networks is that the required length of any one flexure is minimized; however, the imprint of the network hinge is greater than that of a single flexure. Therefore designers must find a compromise between decreased flexure length and hinge imprint.

When analyzing the characteristics of a network hinge the network is modelled as a tessellation of some unit compliant joint with some torsional stiffness (k_θ). The characteristics of the network can then be calculated using the equations for springs in parallel and series. Often, as the network hinge is created by tessellating the same compliant joint, the network can be modelled as a system of equivalent springs combined in series and parallel. For this case the equivalent torsional stiffness of the network (K_θ) is

$$K_\theta = \frac{Pk_\theta}{S} \quad (4.1)$$

where:

k_θ is the torsional stiffness of the unit compliant joint

P is the number of units combined in parallel

S is the number of units combined in series

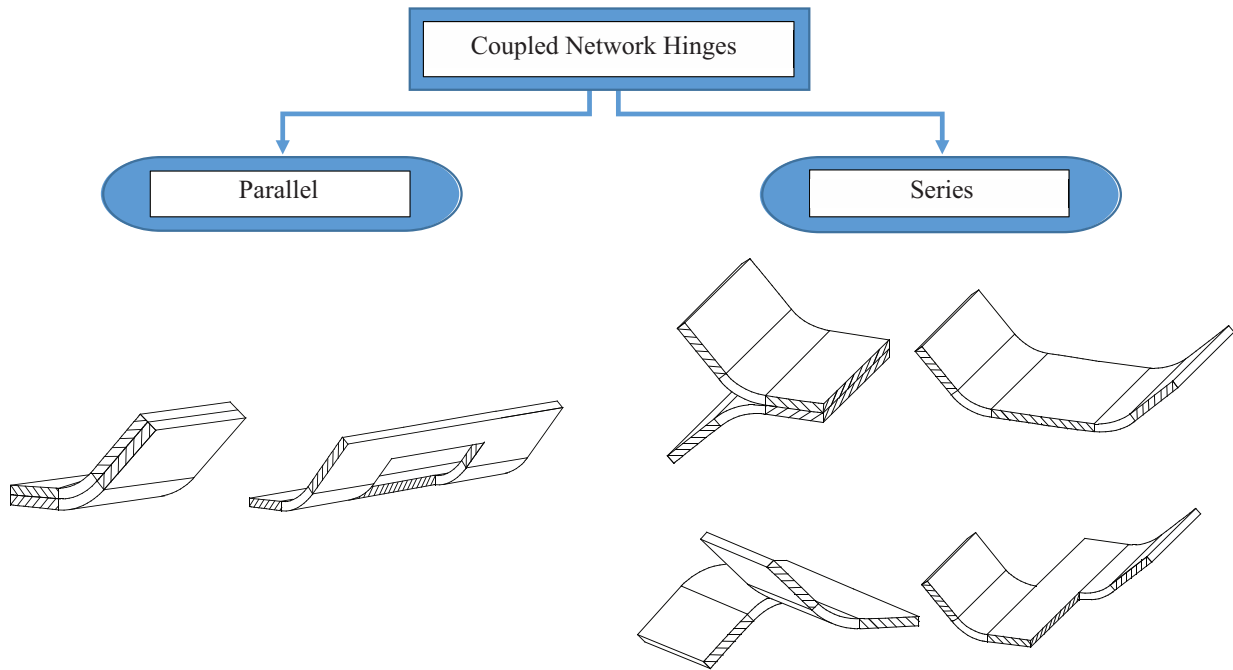


Figure 4.1: Example orientations of network hinges connected in parallel and series. Rigid panels are shown with hash marks and network hinges with solid fill.

While this approach of creating surrogate hinges in metal is effective, it changes the kinematics of the origami-based mechanism. This is due to the fact that the network hinge creates a “distributed hinge”, causing a shift in the center of rotation as the hinge deflects. In applications where it would be essential to maintain the kinematics of the origami model, the panels of the mechanisms would have to be modified (lengthened/shortened/etc.) to account for this shift. Additionally, network hinges that have too large of an imprint may introduce parasitic motions into the final mechanism. This can be resolved by increasing the compliance of the unit joint being tessellated (requiring fewer units and lowering the network’s imprint).

4.4.2 Systems of Network Hinges

Multiple network hinges can be coupled together to further increase the performance of the metal surrogate hinge. Each individual network hinge is connected through a rigid segment to each other (either in parallel or in series). Some possible ways of coupling network hinges in series and parallel are demonstrated in Figure 4.1. Of these, one configuration, shown again in Figure 4.2,

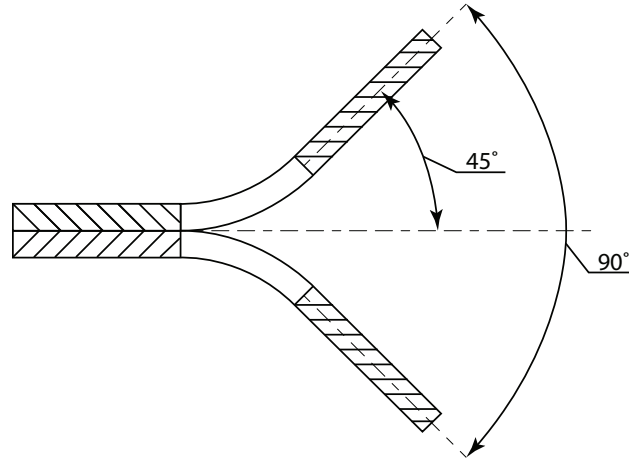


Figure 4.2: Stacked orientation of serially connected network hinges with overall hinge deflection and individual network hinge deflection angles shown.

may be of particular interest to designers of origami-based mechanisms. This stacked orientation creates a new undeflected position (with the panels laying on top of each other rather than adjacent) as well as a hard-stop for the hinge. Further, it more closely approximates an origami paper crease with a fixed axis of rotation.

The use of these systems of network hinges allows designers to further tailor the performance of the surrogate hinge. For instance, connecting network hinges in series effectively lowers the overall stiffness. This can be used by designers to achieve greater deflections (or a given deflection with lower stress in the individual network hinges as demonstrated in Figure 4.2).

4.5 Conclusions

In this chapter the selection of surrogate hinges for use in origami-based mechanisms was explored. Several considerations and their affect on the hinge/mechanism were discussed. Additionally, considerations for the development of surrogate hinges in metals were presented – allowing designers to develop compliant hinges that will be appropriate in mechanisms for use in demanding environments or with large applied loads.

The considerations discussed in the chapter will allow designers of origami-based mechanisms to more effectively select surrogate hinges that will minimize parasitic motions, and ensure that the required performance of the mechanism is met. This is important as the mechanisms’

force-deflection behavior and mechanical advantage are greatly affected by the hinges being used. Increased understanding of this key design parameter, as well as the others controlling the performance of origami-based mechanisms will lead to the creation of origami-based mechanisms with greater performance, capabilities, and application.

CHAPTER 5. CONCLUSION

5.1 Conclusions

This thesis has presented designers of origami-based mechanisms with fundamental knowledge of a developing area of engineering design. While there is great potential for these mechanisms to provide valuable solutions to challenging engineering problems with their unique set of characteristics, this potential is currently limited by lack of design tools, models, or experience specific to origami-based design.

This work enumerated the fundamental motions in origami-based mechanisms - along with required actuation inputs, developed a kinematic model of such mechanisms, and discussed key considerations for the selection of surrogate hinges (including a discussion of the development of these hinges in metals). The information presented herein will help in the proliferation and sophistication of origami-based mechanisms.

While providing useful insight into the critical aspects of origami-based design (such as motions, actuation requirements, and force-deflection behavior), this thesis demonstrated that the kinematic analysis of origami-based mechanisms yields one main advantage: it allows for the development of predictive models and tools that will give designers greater ability to control and optimize the performance of the mechanism being developed (as shown in Chapter 3).

These predictive models allow for the exploration of key parameters controlling the motions and performance of origami-based mechanisms which can in turn be studied in detail. Further, using the predictive models, these parameters can be ranked by their effect on origami-based mechanisms, allowing designers to know just how critical a given aspect of the design may be in achieving the required performance.

5.2 Future Work

As has been stated, the work that was done in this thesis is but a preliminary effort to developing a set of key parameters and guidelines for the the efficient design of origami-based mechanisms. There are three areas in particular that would benefit from further work.

1. A more developed study of origami models and their motions – including more advanced motions and how to combine the fundamental motions already considered to capture arbitrary motions as required.
2. A further developed study of mechanical advantage including a study of origami tessellations as well as non flat-foldable origami patterns and the parameters affecting force transfer and motion propagation such origami fold patterns.
3. Lastly, a kinematic study of origami-based mechanisms with distributed hinges – in order to better understand the effect of network hinges (as discussed in Chapter 4) on the kinematic behavior of the mechanism and how to effectively maintain desired kinematics.

REFERENCES

- [1] Wilcox, E., Magleby, S., and Howell, L., 2014. “Exploring movements and potential actuation in action origami.” In *Proceedings of the ASME 2014 International Design Engineering Technical Conferences and Computers and Information in Engineering Conference*, ASME DETC2014–34428. 2, 27, 41
- [2] Kuribayashi, K., Tsuchiya, K., You, Z., Tomus, D., Umemoto, M., Ito, T., and Sasaki, M., 2006. “Self-deployable origami stent grafts as a biomedical application of ni-rich tni shape memory alloy foil.” *Materials Science and Engineering: A*, **419**(12), pp. 131 – 137. 4, 25, 41
- [3] Baranger, E., Guidault, P.-A., and Cluzel, C., 2011. “Numerical modeling of the geometrical defects of an origami-like sandwich core.” *Composite Structures*, **93**(10), pp. 2504 – 2510. 4, 25
- [4] Zirbel, S., Magleby, S., Howell, L., Lang, R., Thomson, M., and Trease, B., 2013. “Accommodating thickness in origami-based deployable arrays.” *Journal of Mechanical Design*, **135**(11), October, p. 111005. 4, 25
- [5] Ahmed, S., Lauff, C., Crivaro, A., McGough, K., Sheridan, R., Frecker, M., Lockette, P., Ounaies, Z., Simpson, T., Lien, J., and Strzelec, R., 2013. “Multi-field responsive origami structures: Preliminary modelling and experiments.” In *Proceedings of the ASME 2013 International Design Engineering Technical Conferences and Computers and Information in Engineering Conference*, ASME DETC2013–12405. 4
- [6] Leng, J., Lan, X., Liu, Y., and Du, S., 2011. “Shape-memory polymers and their composites: Stimulus methods and applications.” *Progress in Materials Science*, **56**(7), pp. 1077–1135. 4
- [7] Hawkes, E., An, B., Benbernou, N. M., Tanaka, H., Kim, S., Demaine, E. D., Rus, D., and Wood, R. J., 2010. “Programmable matter by folding.” *Proceedings of the National Academy of Sciences of the United States of America*, **107**, pp. 12441–12445. 4, 41
- [8] Bowen, L., Grames, C., Magleby, S., Lang, R., and Howell, L., 2013. “A classification of action origami as systems of spherical mechanisms.” *Journal of Mechanical Design*, **135**(11), October 8, p. 111008. 5, 8, 9, 21, 23, 27
- [9] Winder, B., Magleby, S., and Howell, L., 2009. “Kinematic representations of pop-up paper mechanisms.” *Journal of Mechanisms and Robotics*, **1**(2), pp. 1–10. 5, 26, 42
- [10] Balkcom, D. J., and Mason, M. T., 2008. “Robotic origami folding.” *The International Journal of Robotics Research*, **27**(5), May, pp. 613–627. 5, 26, 42

- [11] Zhang, K., Fang, Y., Dai, J. S., and Fang, H., 2010. “Geometry and constraint analysis of the three-spherical kinematic chain based parallel mechanism.” *Journal of Mechanisms and Robotics*, **2**(3), July 23, p. 031014. 5, 26, 42
- [12] Dureisseix, D., 2012. “An overview of mechanisms and patterns with origami.” *International Journal of Space Structures*, **27**(1), March, pp. 1–14. 5, 26, 42
- [13] Lang, R., 1997. *Origami in Action.*, 1 ed. St. Martin’s Griffin, New York, NY. 9, 11, 20
- [14] Lang, R., 1988. *The Complete Book of Origami.* Dover Publications, Inc, Mineola, NY. 9
- [15] Shafer, J., 2010. *Origami Ooh La La!*. CreateSpace Independent Publishing Platform, Lexington, KY. 9, 11, 20
- [16] Shafer, J., 2001. *Origami to Astonish and Amuse.*, 1 ed. St. Martin’s Griffin, New York, NY. 9
- [17] Douglas, S., Bachelet, I., and Church, G., 2012. “A logic-gated nanorobot for targeted transport of molecular payloads.” *Science*, **335**(6070), February, pp. 831–834. 25
- [18] Nojima, T., and Saito, K., 2006. “Development of newly designed ultra-light core structures.” *JSME International Journal Series A Solid Mechanics and Material Engineering*, **49**(1), pp. 38–42. 25
- [19] Cheng, Q., Song, Z., Ma, T., Smith, B., Tang, R., Yu, H., Jiang, H., and Chan, C., 2013. “Folding paper-based lithium-ion batteries for higher areal energy densities.” *Nano Letters*, **13**(10), pp. 4969–4974. 25
- [20] Onal, C., I. Wood, R. J., and Rus, D., 2031. “An origami-inspired approach to worm robots.” *IEEE Transactions on Mechatronics*, **18**(2), pp. 430–438. 25
- [21] Lee, D.-Y., Koh, J.-S., Kim, J.-S., Kim, S.-W., and Cho, K.-J., 2013. “Deformable -wheel robot based on soft material.” *International Journal of Precision Engineering and Manufacturing*, **14**(8), August, pp. 1439–1445. 25
- [22] Felton, S., Tolley, M., Demaine, E., Rus, D., and Wood, R., 2014. “A method for building self-folding machines.” *Science*, **345**(6197), August, pp. 644–646. 25
- [23] Frecker, M., and Canfield, S., 2000. “Optimal design and experimentation validation of compliant mechanical amplifiers for piezoceramic stack actuators.” *Journal of Intelligent Material Systems and Structures*, **11**, pp. 360–369. 25
- [24] Qiu, C., Aminzadeh, V., and Dai, J., 2013. “Kinematic analysis and stiffness validation of origami cartons.” *Journal of Mechanical Design*, **135**(11), p. N/A. 26, 42
- [25] Evans, T. A., Lang, R. J., Magleby, S. P., and Howell, L. L., 2015. “Rigidly foldable origami twists.” *Origami6* Accepted for Publication. 28, 36
- [26] Lang, R. *Sector/Dihedral Relations.* pp. 262–264 Pending Publication. 29
- [27] Salamon, B., and Midha, A., 1998. “An introduction to mechanical advantage in compliant mechanisms.” *Journal of Mechanical Design*, **120**(2), pp. 311–315. 29

- [28] Hull, T., 2012. *Project Origami.*, 2 ed. A K Peters/CRC Press, Boca Raton, Fl. 32
- [29] Lobontiu, N., 2003. *Compliant Mechanisms: Design of Flexure Hinges.*, 1 ed. CRC Press, Boca Raton, Fl. 39, 42
- [30] Delimont, I., Magleby, S., and Howell, L., 2014. “Evaluating compliant hinge geometries for origami-inspired mechanisms.” In *Proceedings of the ASME 2014 International Design Engineering Technical Conferences and Computers and Information in Engineering Conference*, ASME DETC2014–34376. 39, 42
- [31] Tian, Y., Shirinzadeh, B., Zhang, D., and Zhong, Y., 2010. “Three flexure hinges for compliant mechanism designs based on dimensionless graph analysis.” *Precision Engineering*, **34**(1), January, pp. 92–100. 39, 42
- [32] Qattawi, A., Mayyas, A., Thiruvengadam, H., Kumar, V., Dongri, S., and Omar, M., 2014. “Design considerations of flat patterns analysis techniques when applied for folding 3-d sheet metal geometries.” *Journal of Intelligent Manufacturing*, **25**(1), pp. 109–128. 41
- [33] Saito, K., Pellegrino, S., and Nojima, T., 2014. “Manufacture of arbitrary cross-section composite honeycomb cores based on origami techniques.” *Journal of Mechanical Design*, **136**(5). 41
- [34] Deng, D., and Chen, Y., 2013. “An origami inspired additive manufacturing process for building thin-shell structures.” *ASME 2013 International Mechanical Engineering Congress and Exposition*, **2A**. 41
- [35] Zirbel, S., Wilson, M., Magleby, S., and Howell, L., 2013. “An origami-inspired self-deployable array.” *ASME 2013 Conference on Smart Materials, Adaptive Structures and Intelligent Systems*, **1**. 41
- [36] Daniela, A. B. R., 2014. “Designing and programming self-folding sheets.” *Robotics and Autonomous Systems*, **62**(7), pp. 976–1001. 41
- [37] An, B., Benbernou, N., Demaine, E., and Rus, D., 2011. “Planning to fold multiple objects from a single self-folding sheet.” *Robotica*, **29**(1), pp. 87 – 102. 41
- [38] Ferrell, D., Isaac, Y., Magleby, S., and Howell, L., 2011. “Development of criteria for lamina emergent mechanism flexures with specific application to metals.” *Journal of Mechanical Design*, **133**(3). 42, 43
- [39] Gitlin, B., Kveton, A., and Lalvani, H., 2003. Method of bending sheet metal to form three-dimensional structures, Nov. 4 US Patent 6,640,605. 42
- [40] Russell-Clarke, P., and Nasher, M., 2013. Interlocking flexible segments formed from a rigid material, Aug. 22 US Patent App. 13/768,943. 45